Time Varying Carrier Frequency Offset Estimation in Multicarrier Underwater Acoustic Communication

Gilad Avrashi

Time Varying Carrier Frequency Offset Estimation in Multicarrier Underwater Acoustic Communication

Research Thesis

Submitted in partial fulfillment of the requirements
for the degree of Master of Science in Electrical Engineering

Gilad Avrashi

Submitted to the Senate of the
Technion — Israel Institute of Technology
Tammuz 5780 Haifa July 2020

Acknowledgments

The research thesis was done under the supervision of Prof. Israel Cohen and Dr. Alon Amar in the Department of Electrical Engineering. I would like to express my gratitude to both of them for the supervision, guidance and support throughout all the stages of this research.

I would like to acknowledge Dr. Yaakov Buchris for his guidance and assistance during this research.

I would like to express my deep gratitude to my wife Yael, for the constant love, encouragement and support.

List of Publications

The following papers have been published or submitted for publication based on the results of the work described in this thesis:

- G. Avrashi, A. Amar, and I. Cohen, "Time Varying Carrier Frequency Offset Estimation in Multicarrier Underwater Acoustic Communication", *submitted to MDPI Journal of Marine Science and Engineering.*

- G. Avrashi, A. Amar, I. Cohen, and M. Stojanovic, "Eigenvalue decomposition based estimators of carrier frequency offset in multicarrier underwater acoustic communication", *IEEE ICASSP Conf.*, New Orleans, USA, Mar. 2017.

Contents

List of Figures

Abstract

In this work we consider a group of closed-form carrier frequency offset estimators for multicarrier underwater acoustic communication. Acoustic modems are used for various underwater platforms including environmental monitoring beacons, and autonomous underwater vehicles (AUVs). With a growing need for applications such as image and video streaming, a considerable amount of attention has been given to high bandwidth communication schemes which can handle the dynamic underwater acoustic channel. In the past decade, multicarrier communications have been extensively used for these applications.

Carrier frequency offset (CFO) in orthogonal frequency division multiplexing (OFDM) communication systems may cause inter-carrier interference and degrades the performance of OFDM decoders. Over the past decades, numerous techniques were proposed to estimate frequency offsets in OFDM, focusing mainly on radio communication channels which are quite different from the acoustic channel. The time variations of the underwater acoustic communication (UAC) channel are non-negligible with respect to the propagation speed and are subject to multipath effects, ultimately causing non-uniform Doppler shifts and short coherence time. These variations have encouraged UAC modem designers to use block-by-block frequency estimators which require a grid search in the frequency domain and thus suffer from high computational complexity.

Recently, low complexity CFO estimators for OFDM in the UAC channel have been suggested that replace the need for an exhaustive grid search. Using equi-spaced pilot tones in the frequency domain and setting them to be identical, results in a periodic time-domain block with a period equal to the number of pilot tones. By utilizing this, the problem of estimating the CFO is shown to have a closed-form and can be solved effectively given that it is constant during one block. These estimators, however, suffer from two drawbacks making them hard to implement in practical modems: (1) The use of equi-spaced identical pilots results in high peak to average power ratio (PAPR); (2) The

assumption of having a constant CFO limits the design of the OFDM block.

In this work, we propose a transmitter-receiver design that allows closed-form CFO estimation. Instead of identical pilots, we propose a method for designing the pilot tones, such that the time periodicity feature is preserved while the effect on PAPR is negligible. By looking at pilot design as a phase retrieval problem with a time-domain envelope chosen to satisfy the low PAPR requirement, we are able to derive a tunable design algorithm for the transmitted signal.

For the receiver side, we develop a closed-form time-varying CFO estimator. The method expands the previously developed closed-form CFO estimator, which utilizes only the pilot-independent samples of the OFDM block to a complete scheme which also includes the pilot-dependent part. We then develop estimators that can be adapted to time-varying channels. Numerical simulations indicate that the bit error rate (BER) performance of the OFDM modem is significantly improved by using the proposed method. Furthermore, we show that by applying the proposed pilot-design algorithm, PAPR values are within fractions of dB of the original random pilots design without compromising the CFO estimation scheme.

Abbreviations

BER	Bit error rate
CCDF	Complementary cumulative distribution function
CFO	Carrier frequency offset
CIR	Channel impulse response
EVD	Eigenvalue decomposition
FFT	Fast Fourier transform
GEVD	Generalized eigenvalue decomposition
GSA	Gerchberg-Saxton algorithm
ICI	Inter-carrier interference
LS	Least-squares
MLE	Maximum likelihood estimator
NLS	Nonlinear least-squares
NLSE	Nonlinear least-squares estimator
OFDM	Orthogonal frequency division multiplexing
OLA	Overlap and add
PAPR	Peak to average power ratio
PDR	Pilot to data ratio
QPSK	Quadrature phase-shift keying
RMS	Root mean square
RMSE	Root mean square error
s.t.	Subject to
SNR	Signal-to-noise ratio
UAC	Underwater acoustic communication
ZP	Zero padded

List of Notations

Δx	The discrete derivative of x
$(\cdot)^T$	The transpose operator
$(\cdot)^H$	The Hermitian operator
$\mathbf{x}$	Column vector
$\mathbf{X}$	Matrix
j	The imaginary unit
$\text{diag}(\mathbf{x})$	A diagonal matrix whose main diagonal is $\mathbf{x}$
$\underset{x}{\text{argmin}} f(x)$	The argument x which minimizes the function $f(x)$
$\underset{x}{\text{argmax}} f(x)$	The argument x which maximizes the function $f(x)$
$\arg(\mathbf{x})$	The phase of the complex vector $\mathbf{x}$
$\hat{(\cdot)}$	The estimated parameter or parameters vector
$m \text{mod} n$	The modulo of n in m
$\mathbf{0}_{m \times n}$	A $m \times n$ matrix with all elements equal to 0
$\mathbf{I}_n$	The $n \times n$ identity matrix
$\|\cdot\|^2$	The L_2 norm
ϵ_0	The true normalized carrier frequency offset
ϵ	The unknown normalized carrier frequency offset
$E(\cdot)$	The expected value of a parameter or vector
$(\cdot)^*$	The complex conjugate operator
$\otimes$	The Kronecker product

Chapter 1

Introduction

1.1 Motivation

Underwater acoustic communication (UAC) has been studied in the past decades and has recently enjoyed a growing attention as the need to transmit higher rates for longer distances becomes the bottleneck of an entire industry. Carrier frequency offset (CFO) in orthogonal frequency division multiplexing (OFDM) communication systems may cause inter-carrier interference and degrades the performance of OFDM decoders [8,31]. Over the past decades numerous techniques were proposed to estimate frequency offsets in OFDM, focusing mainly on radio communication channels. These methods can be classified into two categories. The first category of CFO estimators, known as data-aided estimators [19–21,23], rely on pilot symbols which are periodically transmitted. The second category, known as blind estimators, use no additional training data and rely solely on the received OFDM data to estimate the CFO by exploiting statistical characteristics of the measurements such as the cyclic prefix segment [13,27], frequency measurements at null subcarrier [4, 15, 18, 26], second order statistics and high order statistics of frequency measurements [16, 30].

Unlike the radio communication channel, the time variations of the UAC channel are non-negligible with respect to the propagation speed and are subject to multipath effects, ultimately causing non-uniform Doppler shifts [25],[14]. These fast variations of the channel result in short coherence time. On the other hand, the UAC suffers from inherently limited bandwidth which places a lower bound to the block duration. Therefore, limiting the duration of OFDM blocks, in order to not exceed the coherence time [29], has implications on either the system bitrate or its channel robustness [5]. These fast variations have

encouraged UAC modem designers to use block-by-block frequency estimators. Accordingly, a coarse Doppler scale compensation is conducted for the entire package, followed by block-by-block estimation of the residual frequency shifts in each block, disregarding neighbor blocks and their estimations.

Li et al. [14] introduced a nonlinear least-squares (NLS) CFO estimator using equi-spaced pilot symbols in each block, which are also used to estimate the channel impulse response (CIR). The authors also employed the least-squares (LS) principle with null symbols in the frequency domain by introducing a minimum energy optimization criterion. Both methods require a grid search in the frequency domain and thus suffer from a high computational burden on the modem. Carracosa and Stojanovic [7] suggested a block-to-block processing approach for UAC OFDM systems, where the non-uniform phase offset is tracked from one block to the subsequent. Although having the advantage of lower computational complexity, this method requires a fairly slow varying channel over two consecutive OFDM blocks, which limits the design and results in bitrate loss.

Recently, low complexity CFO estimators for OFDM in UAC channel have been suggested [2], that replace the need for exhaustive grid search. Using not only equi-spaced pilot tones in the frequency domain, but also set them to be identical, results in a periodic time-domain block with a period equal to the number of pilot tones. After retaining the non-pilot signal parts of each periodic segment, a small-size correlation matrix between these parts is constructed. The problem of estimating the CFO given this correlation matrix is shown to have a closed form and can be solved effectively given that the CFO is constant during the time of one block. These estimators, however, suffer from two drawbacks making them hard to be implemented in practical modems: (1) The use of equi-spaced identical pilots results in high PAPR. This problem is thoroughly discussed in [2], but a solution is not offered; (2) Like previous CFO estimators the assumption of having a constant CFO remains and limits the design of the OFDM block as investigated in [5].

In order to overcome the time-varying nature of the underwater acoustic channel, differential OFDM was suggested combined with a partial fast Fourier transform (FFT) technique, which aims to dissect the OFDM block into several sections and estimates the channel separately, thus reducing the problem into piecewise constant channels [5]. Han et al. [11] suggested an eigenvalue decomposition to combine the weights of the partial FFT sub-blocks.

Herein, we propose a transmitter-receiver design that allows closed-form CFO estimation based on the methods in [2]. The work offers three main contributions: a) we introduce a generalized scheme which utilizes both pilot and non-pilot samples of the block period in order to achieve improved estimation performance; b) The closed-form CFO estimator presented in [2] has an inherent high PAPR which makes it unusable in practical communication systems. We present a transmitter design that allows to reduce the PAPR while preserving the pilot-tone features required for the CFO estimator; c) We present a CFO estimator for time varying frequency shifts, thus extending the usable block durations (formerly limited by the coherence time) and allowing higher data rates. Furthermore, the proposed method eliminates the need to use overlap-and-add for zero padded (ZP)-OFDM in order to estimate the CFO.

Instead of identical pilots, a method for designing the pilot tones is proposed, such that the time periodicity feature is preserved while the effect on PAPR is negligible. By looking at pilot design as a phase retrieval problem with a time domain envelope chosen to satisfy the low PAPR requirement, we are able to derive a tunable design algorithm for the transmitted signal.

For the receiver side, we develop a closed-form time-varying CFO estimator. The method expands the previously developed closed-form constant CFO estimators [2], where the main idea is that by using identical pilots, the OFDM block becomes a sum of a periodic impulse signal (caused by the pilot tones) and a random signal (caused by the data tones). In the absence of CFO, the sections of the period which do not include the pilot signal or its multipath replicates are uncorrelated (and therefore we use the term noise-space). A group of closed form solution has been suggested in order to estimate the frequency offset that minimizes the noise-space correlation over the block. In this work we propose to utilize the correlation between the pilot parts of the period (signal space) which is expected to receive maximal value in the absence of CFO. We then combine between both methods and utilize all block samples for the estimation. Lastly, we show that, under certain conditions, these estimators can be adapted to time-varying channels. Numerical simulations indicate that, for time varying channels, the BER performance of the OFDM modem is significantly improved by using the proposed method. Furthermore, we show that by applying the proposed pilot-design algorithm, PAPR values within fractions of dB of the original random pilots design without compromising the CFO estimation scheme.

1.2 A Constrained Optimization for Pilots Design

We start by solving the transmitter side drawback of the closed-form CFO estimator making the method impractical for deployment in the underwater environment. We start by investigating the effect of the pilot tone design on both the resulting PAPR and the applicability of the closed form estimator, ranging from constant to random pilot tones. We show that these two aspects are somewhat contradicting, meaning that trying to design the pilot tones such that the resulting PAPR is low results in reduced CFO estimation performance and vice versa.

In order to solve this trade-off, we develop a closed-form iterative algorithm for pilot tone design. As the pilot tones are required to have unit amplitude in order to maintain a simple channel equalizer, the proposed algorithm is required to design only the pilot tone phases while producing a time domain signal which will compromise between low PAPR and the desired time locality for the CFO estimator. The problem of setting the phases of a frequency domain signal in order to achieve a desired envelope in the time domain is known as a phase retrieval problem, which has been studied in the past few decades in various fields. Hereon, we use a generalization of the Gerchberg-Saxton algorithm (GSA), called the error reduction algorithm [6], to reconstruct the pilot phases in the transmitter side. This algorithm is also applied in phase retrieval problems.

1.3 Signal Space Estimation

We first present an equivalent method for the noise-space estimation. Instead of using the non-pilot parts, we use the samples containing pilot tone and pilot tone replicas of each period in order to construct a correlation matrix. The eigenvector associated with the maximal eigenvalue of this matrix is used to estimate the phase accumulations between the pilot-signal periods, and then the CFO is estimated using a linear LS estimator given the phases accumulations.

We then develop two closed-form CFO estimators which combines the noise-space and signal-space matrices. The first is a weighted linear LS estimator, given the phases of the minimal eigenvector of the noise-space correlation matrix and the maximal eigenvector of the signal-space correlation matrix. The second estimator solves a generalized eigenvalue decomposition (GEVD) problem by considering jointly the two correlation matrices and then performing a similar second step as the previous estimators.

1.4 Time-Varying CFO Estimation

We expand the closed-form work-frame to support estimation of time-varying CFO within the OFDM block. The time variations observable are limited to the number of periods of the pilot signal. Therefore, we describe two model-based estimation schemes. The first, assumes that the CFO temporal changes can be approximated as a polynomial function. The second, approximates a piecewise constant temporal behavior.

Both methods are developed under slow-variation and small-variation assumptions, which in some environments will not hold. However, it provides a tool to adjust the modem parameters and increase communications throughput by using prior knowledge of the acoustic channel.

1.5 Problem Statement and Model Assumptions

Consider a zero-padded orthogonal frequency multiplexing (ZP-OFDM) block with time duration T and K carriers, where the kth carrier frequency is

$$f(k) = f_0 + k\Delta f\,, k = 0, \ldots, K-1\,, \tag{1.1}$$

with f_0 the lower frequency, and $\Delta f = 1/T$ is the carrier spacing. Let the $K \times 1$ vector of symbols be

$$\mathbf{s} = [s(0), s(1), \ldots, s(K-1)]^T\,, \tag{1.2}$$

where $s(k) = e^{j\phi(k)}$. The K carriers are composed of $K-Q \gg Q$ data symbols with $\phi(k) \in \mathcal{S}$ and $\mathcal{S}$ is a pre-defined set of phases (such as the quadrature phase-shift keying (QPSK) constellation). The remaining Q symbols are used as pilots, equi-spaced in frequency with spacing $G = K/Q$, i.e., according to (1.1) the frequency of the qth pilot carrier is $f(qG)$, $q = 0, 1, \ldots, Q-1$. The $P \times 1$ zero-padded discrete time transmitted signal, where $P = K + L$, is

$$\mathbf{r} = \mathbf{T}_{zp}\mathbf{F}_K^H\mathbf{s}\,, \tag{1.3}$$

where $\mathbf{F}_K$ is a $K \times K$ Fourier matrix with the (m,n)th element given by $\frac{1}{\sqrt{K}}e^{-j2\pi/K \cdot mn}$, $\mathbf{T}_{zp} = [\mathbf{I}_K, \mathbf{0}_K\mathbf{0}_L^T]^T$ is a $P \times K$ zero-padding matrix, $\mathbf{I}_n$ is the $n \times n$ identity matrix, $\mathbf{0}_n$ is a $n \times 1$ vector of zero elements, and L is the length of zero-padding. We assume that the unknown discrete-time baseband CIR represents a multipath channel which introduces

frequency-dependent Doppler effect. The latter is commonly compensated in the receiver using a packet preamble which is used for estimation and rescaling of the time axis [14]. Hereon, we look at the OFDM blocks after this compensation, which means that we deal with a multipath channel described by the $L \times 1$ vector

$$\mathbf{h} = [h(0), h(1), \ldots, h(L-1)]^T , \tag{1.4}$$

where L is the delay spread of the channel normalized by the sampling interval,[1] $T_s = T/K$. It is assumed that the $P \times 1$ received vector $\mathbf{y} = [y(0), \ldots, y(P-1)]^T$ may still consist of a frequency independent residual Doppler shift component which has the following structure [14, 22]

$$\mathbf{y} = \underbrace{\mathbf{\Gamma}_P(\epsilon_0)\mathbf{H}\mathbf{r}}_{\triangleq \mathbf{y}_0} + \mathbf{n} , \tag{1.5}$$

where $\mathbf{y}_0$ is the noise-free received signal, $\mathbf{H}$ is a $P \times P$ Toeplitz matrix with first column and first row given by $[\mathbf{h}^T, \mathbf{0}_{P-L}^T]^T$ and $[h(0), \mathbf{0}_{P-1}^T]^T$, respectively, $\mathbf{n} = [n(0), n(1), \ldots, n(P-1)]^T$ is a $P \times 1$ vector representing the additive noise, which we assume is modeled as a zero-mean circular complex white Gaussian with covariance matrix $\sigma_n^2 \mathbf{I}_P$. Also, we define the normalized CFO, ϵ_0 as the physical frequency offset relative to the carrier spacing, Δf. Accordingly, the $P \times P$ matrix $\mathbf{\Gamma}_P(\epsilon_0)$ is defined as

$$\mathbf{\Gamma}_P(\epsilon_0) = \mathrm{diag}(1, e^{j2\pi\frac{\epsilon_0}{K}}, \ldots, e^{j2\pi\frac{\epsilon_0}{K}(P-1)}) . \tag{1.6}$$

Notice that in this formulation, the CFO is assumed to be constant. In practice this approximation may not hold, thus the formulation will include $\epsilon[n]$, $n = 0, \ldots, P-1$ instead of ϵ_0. The problem herein is: Given P samples of the received OFDM block, $\mathbf{y}$, estimate the unknown parameter vector, $\epsilon[n]$.

1.6 Thesis Structure

This thesis is organized as follows. In Chapter 2 we briefly review methods for estimating CFO used in this work. In Chapter 3 we expand the previously developed closed-form CFO estimator to include the so-called signal-space samples and thus increasing its performance. While the previous method had solved an optimization problem defined for the noise-space

[1] In practice, prior measurements indicate the delay spread of the channel and we can set the CIR length to L. Thus, to avoid inter-block interference, we set the zero padding length equal to the channel length.

(in this case the OFDM data samples) solely, we also use the signal-space (pilot samples) in order to define a combined optimization problem. In Chapter 4 we solve the problem of high PAPR introduced by the pilot-tone design of the closed-form CFO estimator. We define the pilot-tone design as a phase retrieval problem and propose an iterative algorithm which solves it. In Chapter 5 we propose a closed-form CFO estimation scheme which is adapted for time-varying frequency offsets. By utilizing the sub-block segments introduced by the time domain pilot signal, we propose a model based technique fir sub-block CFO estimation. Finally, in Chapter 6 we conclude the work and suggest some future research directions.

Chapter 2

Background

2.1 Introduction

In this chapter we present a brief review of CFO estimation methods in multicarrier underwater acoustic communication modems. There are countless methods for estimating the frequency offset in OFDM receivers. Here, we focus on those who are related to this research and have been a foundation of our work. As presented in Section 1.5, all methods deal with the CFO as a narrowband problem. It is assumed that prior to the CFO estimation a coarse Doppler compensation is performed such that the remaining frequency shift is smaller such that the resulting time-domain rescaling does not exceed the sampling interval, i.e. $\epsilon < 1$.

2.2 Non-linear Least Squares Blind Estimation

The NLS blind estimation method was introduced by Li et al for underwater acoustic OFDM. It uses null subcarriers and performs a grid search in the receiver side over the null subcarriers set. It requires no prior knowledge and performs a block-by-block estimation. Consider a sub-set of the block subcarriers denoted by $\mathcal{S}_N$, notice that null and pilot subcarriers shall not overlap as to avoid the effect on channel estimation. The received signal $\mathbf{y}$ is pre-multiplied by the hypothesized CFO compensation matrix $\tilde{\mathbf{\Gamma}}_P(\epsilon)$, where,

$$\tilde{\mathbf{\Gamma}}_P(\epsilon) = \mathrm{diag}(1, e^{j2\pi\frac{\epsilon}{K}}, \ldots, e^{j2\pi\frac{\epsilon}{K}(P-1)}) \,. \tag{2.1}$$

For each subcarrier, $m \in \mathcal{S}_N$, we calculate the resulting energy, and then summing the energies of all null subcarriers, by performing:

$$J(\epsilon) = \sum_{m \in \mathcal{S}_N} \left| \mathbf{f}_m^H \tilde{\mathbf{\Gamma}}_P^H(\epsilon) \mathbf{y} \right|^2 , \tag{2.2}$$

where $\mathbf{f}_m = [1, e^{j2\pi m \frac{1}{K}}, \ldots, e^{j2\pi m \frac{P-1}{K}}]^T$. If the receiver compensates the data samples with the correct CFO, the null subcarriers will not see the inter-carrier interference (ICI) spilled over from neighboring data subcarriers. Hence, an estimate of can be found through

$$\hat{\epsilon} = \underset{\epsilon}{\operatorname{argmin}} J(\epsilon) , \tag{2.3}$$

which requires an exhaustive search.

2.3 Synchronization Blocks

Synchronization blocks methods have been in use for radio communications in the past few decades [12]. The underlying principle of these methods is that the frequency estimation problem can be reduced to a phase estimation problem by considering the phase shift between two subsequent OFDM blocks. Given that the data $\mathbf{r}$ is known for the two blocks, the phase can be estimated by extracting the angle of the correlation function between the blocks,

$$\begin{aligned} \hat{\epsilon} &= \frac{K}{2\pi P} \arg \left\{ \mathbf{y}_l^H \mathbf{y}_{l+1} \right\} \\ &= \frac{K}{2\pi P} \arg \left\{ \mathbf{r}^H \mathbf{H}^H \mathbf{\Gamma}_{P,l}^H(\epsilon_0) \mathbf{\Gamma}_{P,l+1}(\epsilon_0) \mathbf{H} \mathbf{r} + \mathbf{n}_l^H \mathbf{n}_{l+1} \right\} \\ &\cong \frac{K}{2\pi P} \arg \left\{ \mathbf{\Gamma}_{P,l}^H(\epsilon_0) e^{j2\pi \frac{\epsilon_0}{K} P} \mathbf{\Gamma}_{P,l}(\epsilon_0) \right\} \\ &= \epsilon_0 . \end{aligned} \tag{2.4}$$

This simple operation can be done in various versions. In the general case [19], we can chose blocks which are separated by $D-1$ unknown data blocks (for subsequent blocks $D = 0$). In [8] Classen and Meyr suggested using blocks with both unknown data and known pilot subcarriers. In this case, the pilot tones should be extracted before calculating the correlation,

$$\hat{\epsilon} \cong \frac{K}{2\pi DP} \arg \left\{ \sum_{m \in \mathcal{S}_P} (\mathbf{f}_m^H \mathbf{y}_l)^* (\mathbf{f}_m^H \mathbf{y}_{l+D-1}) \right\} . \tag{2.5}$$

2.4 Identical Pilots Low-Complexity Estimation

The third method discussed hereon performs a block-by-block CFO estimation as in the case of the described NLS blind estimation in Section 2.2, while avoiding the exhaustive grid search. A group of low-complexity closed-form CFO estimators has been proposed in [2].

First, the following observation is made: the transmitted time domain signal can be decomposed into a known pilot tone and unknown data tone signals,

$$x(n) = \underbrace{\sum_{k\in\mathcal{S}_P} \frac{1}{\sqrt{K}} s(k) e^{j\frac{2\pi}{K}nk}}_{\triangleq s_p(n)} + \underbrace{\sum_{k\in\mathcal{S}_D} \frac{1}{\sqrt{K}} s(k) e^{j\frac{2\pi}{K}nk}}_{\triangleq \eta(n)}, \tag{2.6}$$

where $|s(k)| = 1$, and $\mathcal{S}_P$, $\mathcal{S}_D$ are the index sets of the pilot and data tones respectively. For equi-spaced pilots $\mathcal{S}_P = \{k : k \mod G = 0\}$ and

$$s_p(n) = \sum_{q=0}^{Q-1} \frac{1}{\sqrt{K}} s(qG) e^{j\frac{2\pi}{Q}nq}, \tag{2.7}$$

which is a Q-periodic signal. The random data related signal, $\eta(n)$, is treated as noise. It has been shown [2] that for $K \gg Q$ it is distributed as white Gaussian noise with $\eta(n) \sim \mathcal{N}(0, \frac{K-Q}{K})$. At this point, the OFDM signal, $x(n)$, is segmented into G segments of Q samples. Notice that the pilot signal is correlated while the so-called data originated noise is uncorrelated between any two segments. By using this feature of the signal, the commonly used estimator can by applied, where a repeated signal is correlated in order to estimate the frequency offset [19].

In [2] it has been proposed to use the constant pilot tone, $s(qG) = e^{j\phi_0}$, where ϕ_0 is some real number, to obtain

$$\begin{aligned} x(n) &= \sum_{q=0}^{Q-1} \frac{1}{\sqrt{K}} e^{j\phi_0} e^{j\frac{2\pi}{Q}nq} + \eta(n) \\ &= \frac{Qe^{j\phi_0}}{\sqrt{K}} \delta[n \bmod Q] + \eta(n) \end{aligned} \tag{2.8}$$

for $n = 0, \ldots, K-1$, where

$$\delta[n] = \begin{cases} 1, & n = 1 \\ 0, & \text{otherwise} \end{cases}. \tag{2.9}$$

We introduce the following assumption: The system design guarantees that there is no pilot signal leakage from one section to the consecutive, in the constant pilot tone setup, this translates to $L+1<Q$. Specifically, it is guaranteed that the ZP section, $\mathbf{y}(K:K+P)$, holds only data-signal paths with no pilot remains. As the CFO estimator treats the data signal as noise, it is beneficial, for this purpose only, to discard the ZP section. Therefore, instead of conducting the standard overlap-and-add operation for ZP-OFDM [22], we simply use the first K taps given by

$$\tilde{\mathbf{y}} = \mathbf{T}_K \mathbf{\Gamma}_K(\epsilon_0)\mathbf{H}\mathbf{r} + \mathbf{T}_K \mathbf{n} \tag{2.10}$$

instead of (1.5), where the trimming matrix T_K is defined as

$$\mathbf{T}_K = [\mathbf{I}_K, \mathbf{0}_{K\times L}]\,. \tag{2.11}$$

The received OFDM signal is CFO compensated by pre-multiplying it by $\mathbf{\Gamma}_K^H(\epsilon)$ for the hypothesized offset ϵ. The compensated block is then transformed to the frequency domain where the pilot carriers are extracted to obtain the $Q\times 1$ hypothesized output vector

$$\mathbf{x}(\epsilon) = \mathbf{T}_{sc}\mathbf{F}_K \mathbf{\Gamma}_K^H(\epsilon)\tilde{\mathbf{y}}\,, \tag{2.12}$$

where $\mathbf{T}_{sc} = \mathbf{I}_K(1:G:K,:)$ selects the pilot tones. Substituting (1.5) into (2.12) when $\epsilon \cong \epsilon_0$ (meaning that the hypothesized and true offsets are close) implies that $\mathbf{x}(\epsilon)$ can be approximated as

$$\mathbf{x}(\epsilon) \cong \sqrt{Q}\mathbf{D}_p \mathbf{F}_Q(:,1:L)\mathbf{h} + \boldsymbol{\eta}\,, \tag{2.13}$$

where $\mathbf{h}$ is the $L\times 1$ CIR, $\mathbf{D}_p$ is a $Q\times Q$ diagonal matrix containing the pilot symbols on its diagonal, $\mathbf{F}_Q(:,1:L)$ is obtained by taking the first L columns of the $Q\times Q$ Fourier transform matrix and $\boldsymbol{\eta}$ is a zero-mean WGN. In order to determine ϵ and $\mathbf{h}$, a NLS optimization problem is defined, where the estimated values minimize the Euclidean squared distance between $\mathbf{x}(\epsilon)$ and its approximation in (2.13), i.e.,

$$L(\epsilon,\mathbf{h}) = \|\mathbf{x}(\epsilon) - \sqrt{Q}\mathbf{D}_p \mathbf{F}_Q(:,1:L)\mathbf{h}\|^2\,. \tag{2.14}$$

Taking the derivative of (2.14) with respect to (w.r.t.) $\mathbf{h}$ and equating the result to zero,

yields the LS estimate of the CIR:

$$\hat{\mathbf{h}} = \frac{1}{\sqrt{Q}}\mathbf{F}_Q^H(:, 1:L)\mathbf{D}_p^H\mathbf{x}(\epsilon)\,. \tag{2.15}$$

Substituting (2.15) into (2.14) implies that the estimate of the CFO is obtained by selecting ϵ that minimizes the quadratic form

$$\ell(\epsilon) = \mathbf{x}^H(\epsilon)\mathbf{D}_p(\mathbf{I}_Q - \mathbf{F}_Q(:, 1:L)\mathbf{F}_Q^H(:, 1:L))\mathbf{D}_p^H\mathbf{x}(\epsilon). \tag{2.16}$$

It has been shown [2] that $\mathbf{x}(\epsilon)$ can be expressed using a segmented version of the received signal given as

$$\mathbf{Y} = [\mathbf{y}(1:Q), \cdots, \mathbf{y}(K-Q+1:K)]\,, \tag{2.17}$$

which means that $\mathbf{Y}$ is a $Q \times G$ matrix obtained by arranging the Q-samples segments of $\mathbf{y}$ in its columns. Using this formulation, (2.12) becomes

$$\mathbf{x}(\epsilon) = \mathbf{F}_Q\mathbf{\Gamma}_Q^H(\epsilon)\mathbf{Y}\boldsymbol{\alpha}(\epsilon)\,, \tag{2.18}$$

where $\mathbf{F}_Q$ is the $Q \times Q$ Fourier transform matrix, $\mathbf{\Gamma}_Q(\epsilon) = \mathrm{diag}(1, e^{\frac{j2\pi\epsilon}{Q}}, \ldots, e^{\frac{j2\pi\epsilon}{Q}(Q-1)})$, and

$$\boldsymbol{\alpha}(\epsilon) = [1, \ldots, e^{-j\frac{2\pi}{G}(G-1)\epsilon}]^T \tag{2.19}$$

is a $G \times 1$ vector holding the phase accumulations between the different segments such that $\mathbf{\Gamma}_K(\epsilon) = \mathrm{diag}(\boldsymbol{\alpha}^H(\epsilon)) \otimes \mathbf{\Gamma}_Q(\epsilon)$ where $\otimes$ is the Kronecker product. By replacing (2.18) into (2.16) the following form is obtained

$$\ell(\epsilon) = \|\mathbf{Y}\boldsymbol{\alpha}(\epsilon)\|^2 - \|\mathbf{F}_Q^H(:, 1:L)\mathbf{D}_p^H\mathbf{F}_Q\mathbf{\Gamma}_Q^H(\epsilon)\mathbf{Y}\boldsymbol{\alpha}(\epsilon)\|^2\,. \tag{2.20}$$

It has been shown ([2] and see the generalized analysis in section 4.2) that by using identical pilot tones, (2.20) simplifies to the following cost function

$$\ell(\epsilon) = \|\mathbf{Y}(L+1:Q, :)\boldsymbol{\alpha}(\epsilon)\|^2\,, \tag{2.21}$$

The eigenvalue decomposition (EVD)-based estimate consists of two steps. First, from

(1.5) and the definition of $\mathbf{Y}$ in (2.17), the following is obtained

$$\mathbf{Y}(L+1:Q,:) = \mathbf{Y}_0 + \mathrm{N}\,, \tag{2.22}$$

where $\mathbf{Y}_0$ and N are defined similar to $\mathbf{Y}$ for the vectors $\mathbf{y}_0$, $\mathbf{n}$ and then truncated to their last $Q-L$ rows. Substituting (2.22) into (2.21) and unfolding the norm yields

$$\ell_1(\epsilon) = \boldsymbol{\alpha}^H(\epsilon) \left[\underbrace{\mathbf{Y}_0^H \mathbf{Y}_0}_{\mathbf{R}_0} + \mathrm{N}^H\mathrm{N} \right] \boldsymbol{\alpha}(\epsilon)\,. \tag{2.23}$$

Since $\mathrm{N}^H\mathrm{N}$ describes the sample covariance matrix of a white Gaussian noise with variance σ_n^2, the cost function becomes [1]

$$\ell_1(\epsilon) = \boldsymbol{\alpha}(\epsilon)^H \left[\underbrace{\mathbf{R}_0 + \sigma_n^2 \mathbf{I}_G}_{\hat{\mathbf{R}}} \right] \boldsymbol{\alpha}(\epsilon)\,. \tag{2.24}$$

Obviously, using $\mathbf{R}_0$ in place of $\hat{\mathbf{R}}$ in (2.24) yields that $\ell_1(\epsilon) = 0$ for $\boldsymbol{\alpha}(\epsilon) = \boldsymbol{\alpha}(\epsilon_0)$. This means that $\boldsymbol{\alpha}(\epsilon_0)$ is an eigenvector of $\mathbf{R}_0$ corresponding to the zero eigenvalue. In [2] it is proven that this is the minimal eigenvalue of $\mathbf{R}_0$ with probability one. Consequentially, the minimal eigenvalue of $\hat{\mathbf{R}}$ is σ_n^2 and the following relation between the eigenvectors exists,

$$\mathbf{u}_{\min}(\hat{\mathbf{R}}) \cong \mathbf{u}_{\min}(\mathbf{R}_0) + \delta\mathbf{u}_{\min}\,, \tag{2.25}$$

where $\mathbf{u}_{\min}(\mathbf{A})$ is the eigenvector of the matrix $\mathbf{A}$ corresponding to the smallest eigenvalue. Also, $\delta\mathbf{u}_{\min}$ is a small perturbation with zero mean. Since for the noiseless version $\mathbf{R}_0$ the minimal eigenvalue is simply $\boldsymbol{\alpha}(\epsilon_0)$, a closed form estimate will be

$$\hat{\boldsymbol{\alpha}}(\epsilon_0) = \mathbf{u}_{\min}(\hat{\mathbf{R}}) - \delta\mathbf{u}_{\min}\,. \tag{2.26}$$

The second step of the EVD estimation will be extracting the CFO ϵ_0. This is done by observing the phase of (2.26) given by

$$-\frac{2\pi}{G}\mathbf{g}\epsilon_0 \cong \arg(\mathbf{u}_{\min}(\hat{\mathbf{R}})) - \arg(\delta\mathbf{u}_{\min})\,, \tag{2.27}$$

[1] An intuitive approach to the described EVD based CFO estimate comes from the field of sensor array processing. We can consider ϵ as the direction of a arrival of the desired signal, and $\boldsymbol{\alpha}(\epsilon)$ as a steering vector. The EVD solution is then analogous to a minimum variance beamformer.

where $\mathbf{g} = [0, 1, \ldots, G-1]^T$. Finally, the closed form estimate is given by the LS solution of the problem formulated in (2.27),

$$\hat{\epsilon} = -\frac{G}{2\pi} \cdot \frac{\sum_{g=0}^{G-1} g[\arg(\mathbf{u}_{\min}(\hat{\mathbf{R}}))]_g}{\sum_{g=0}^{G-1} g^2}. \tag{2.28}$$

This result requires a EVD of a $G \times G$ matrix followed by a simple linear combination of a $G \times 1$ vector.

2.5 Discussion

In this chapter we have reviewed three methods for estimating the CFO in multicarrier communications. The Blind NLS estimator has the advantage of estimating the CFO block-by-block and thus allowing it to change between the blocks, however it suffers from high computational complexity as it requires a grid search. On the other hand, the synchronization blocks method is very simple and has low computational complexity, however when considering UAC, it is rarely guaranteed that the CFO will remain the same between subsequent blocks, which make this method impractical for the acoustic channel. The identical pilots estimators are both block-by-block and have low computational complexity. Although showing some promising results, these methods suffer from 2 drawbacks, making them impractical: a) They introduce high PAPR, and b) they require a time-constant frequency offset, assuming that it holds for the complete duration of the OFDM block. In other words, this solution assumes that the CFO is time-invariant during the OFDM block. In practical underwater acoustic channels, this may not hold.

Chapter 3

Signal Space Estimation

3.1 Introduction

In this chapter we consider an extended algorithm of the EVD based closed-form technique. We first present an equivalent method for the noise-space estimation. Instead of using the non-pilot parts, we use the samples containing pilot tone and pilot tone replicas of each period in order to construct a correlation matrix. The eigenvector associated with the maximal eigenvalue of this matrix is used to estimate the phase accumulations between the pilot-signal periods, and then the CFO is estimated using a linear LS estimator given the phases accumulations.

We then develop two closed-form CFO estimators which combines the noise-space and signal-space matrices. The first is a weighted linear LS estimator, given the phases of the minimal eigenvector of the noise-space correlation matrix and the maximal eigenvector of the signal-space correlation matrix. The second estimator solves a generalized eigenvalue decomposition (GEVD) problem by considering jointly the two correlation matrices and then performing a similar second step as the previous estimators.

3.2 Efficient Time Domain Estimation

We start by exploring the time domain features of the identical pilot OFDM block. In this case the time domain signal is,

$$\tilde{s}(n) = \frac{Qu}{\sqrt{K}}\delta[n \bmod Q] + \eta(n)\,, n = 0, 1, \ldots, K-1\,. \tag{3.1}$$

The resulting signal in the receiver input (1.5) is,

$$\mathbf{y} = \frac{Qu}{\sqrt{K}}\mathbf{\Gamma}_K(\epsilon_0)\mathbf{H}\mathbf{T}_{zp}\boldsymbol{\delta}_{n\bmod Q} + \underbrace{\mathbf{\Gamma}_K(\epsilon_0)\mathbf{H}\mathbf{T}_{zp}\boldsymbol{\eta} + \mathbf{n}}_{\boldsymbol{\chi}}, \tag{3.2}$$

where $\boldsymbol{\chi}$ is white Gaussian as a sum of two white Gaussian vectors. Notice that the time domain pilot signal is Q samples periodic, therefore we divide $\mathbf{y}$ into G sections of Q samples each, $\mathbf{y} = [\mathbf{y}_0^T, \mathbf{y}_1^T, \ldots, \mathbf{y}_{G-1}^T]^T$. Using (3.2), it can be shown that

$$\begin{aligned}\mathbf{y}_g &= \frac{Qu}{\sqrt{K}}\mathbf{\Gamma}_Q(\epsilon_0)\mathbf{h}_Q\alpha_g(\epsilon_0) + \boldsymbol{\chi}_g \\ &= \frac{Qu}{\sqrt{K}}\mathbf{\Gamma}_L(\epsilon_0)\mathbf{h}_Q\alpha_g(\epsilon_0) + \boldsymbol{\chi}_g \quad , \quad g = 0, \ldots, G-1\,,\end{aligned} \tag{3.3}$$

where $\mathbf{\Gamma}_Q$ is obtained by taking the $Q \times Q$ top left block of $\mathbf{\Gamma}_K$, $\alpha_g(\epsilon_0) = e^{-j\frac{2\pi}{G}g\epsilon_0}$, $\mathbf{h}_Q = [\mathbf{h}, 0, \ldots, 0]^T$ is the $Q \times 1$ vector containing the CIR $\mathbf{h}$ in its first L samples [1], and $\boldsymbol{\chi}_g = \chi[(g-1)Q + 1 : gQ]$. The last $Q - L$ samples of $\mathbf{y}_g$ do not contribute to the pilot signal, therefore in the transition we have replaced it by an $L \times 1$ vector, where $\mathbf{\Gamma}_L$ is defined similarly to $\mathbf{\Gamma}_Q$. Using this notation we arrive to the $GL \times 1$ measurement vector,

$$\mathbf{y} = \underbrace{\frac{Qu}{\sqrt{K}}\left[(\mathbf{\Gamma}_L\alpha_0)^T, (\mathbf{\Gamma}_L\alpha_1)^T, \cdots, (\mathbf{\Gamma}_L\alpha_{G-1})^T\right]^T}_{\mathbf{R}(\epsilon_0)}\mathbf{h} + \boldsymbol{\chi}\,. \tag{3.4}$$

At this point we can formulate a LS problem. Given the measurement $\mathbf{y}$, we want to find the CIR, $\mathbf{h}$, and the CFO, ϵ, that minimize the cost function

$$L(\epsilon, \mathbf{h}) = \|\mathbf{y} - \mathbf{R}(\epsilon)\mathbf{h}\|^2\,. \tag{3.5}$$

The CIR estimate is therefore,

$$\hat{\mathbf{h}} = [\mathbf{R}^H(\epsilon)\mathbf{R}(\epsilon)]^{-1}\mathbf{R}^H(\epsilon)\mathbf{y}\,. \tag{3.6}$$

[1] ZP-OFDM receiver schemes use overlap-and-add (overlap and add (OLA)). i.e. the last L elements of the $P \times 1$ vector $\mathbf{y}$ are added to the first elements to create a $K \times 1$ vector. By doing so, the measurement vector can be treated as a cyclic convolution between the transmitted block and the CIR. Notice that when estimating the CIR using identical pilots, the latter L elements of $\mathbf{y}$ do not hold any relevant data (furthermore it decreases the pilot-data ratio), therefore instead of OLA we simply disregard the ZP samples. This can also be done in [2], since the first L elements of each segment are not used for the CFO estimation

Replaced back into (3.5), the estimated CFO is one that maximizes the cost function,

$$\ell(\epsilon) = \|\mathbf{P}_R(\epsilon)\mathbf{y}\|^2 \,, \tag{3.7}$$

where

$$\mathbf{P}_R(\epsilon) = \mathbf{R}(\epsilon)[\mathbf{R}^H(\epsilon)\mathbf{R}(\epsilon)]^{-1}\mathbf{R}^H(\epsilon) \,. \tag{3.8}$$

Replacing (3.4) into the cost function, we obtain,

$$\ell(\epsilon) = \|\mathbf{P}_R(\epsilon)\mathbf{y}\|^2 = \mathbf{y}^H\mathbf{P}_R(\epsilon)\mathbf{y} \,. \tag{3.9}$$

Using the definition of $\mathbf{P}_R(\epsilon)$, we arrive to the time domain channel-free cost function,

$$\ell(\epsilon) = \boldsymbol{\alpha}^H(\epsilon)\mathbf{Y}^H\mathbf{Y}\boldsymbol{\alpha}(\epsilon) \tag{3.10}$$

where $\mathbf{Y} = [\mathbf{y}_0, \ldots, \mathbf{y}_{G-1}]$ and $\boldsymbol{\alpha} = [\alpha_0, \ldots, \alpha_{G-1}]^T$. Notice that using (3.3), $\mathbf{Y}^H\mathbf{Y} = \frac{Q^2}{K}\|\mathbf{h}\|^2\boldsymbol{\alpha}^*(\epsilon_0)\boldsymbol{\alpha}^T(\epsilon_0)$ which means that it has only one non-zero eigenvalue $\lambda = \frac{Q^2}{K}\|\mathbf{h}\|^2$ with a corresponding eigenvector $\mathbf{v} = \boldsymbol{\alpha}^*(\epsilon_0)$. Keeping this in mind, we rephrase the optimization problem as follows,

$$\hat{\mathbf{w}}(\epsilon) = \operatorname{argmax} \mathbf{w}^H(\epsilon)\mathbf{Y}^H\mathbf{Y}\mathbf{w}(\epsilon) \quad \text{s.t.} \quad \mathbf{w}^H(\epsilon)\mathbf{w}(\epsilon) = 1 \,, \tag{3.11}$$

or equivalently,

$$\hat{\mathbf{w}}(\epsilon) = \underset{\mathbf{w}(\epsilon)}{\operatorname{argmax}} \frac{\mathbf{w}^H(\epsilon)\mathbf{Y}^H\mathbf{Y}\mathbf{w}(\epsilon)}{\mathbf{w}^H(\epsilon)\mathbf{w}(\epsilon)} \,, \tag{3.12}$$

which is a simple Rayleigh quotient and therefore $\mathbf{w}(\hat{\epsilon})$ that solves the maximization problem is the eigenvector corresponding to the maximal eigenvalue of $\mathbf{Y}^H\mathbf{Y}$. Finally, the CFO estimate is achieved by solving the LS problem

$$\underset{\epsilon}{\operatorname{argmin}} \| \arg \mathbf{v} + \frac{2\pi}{G}\epsilon\mathbf{g}\|^2 \,, \tag{3.13}$$

where $\mathbf{g} = [0, 1, \ldots, G-1]^T$ to obtain the estimate

$$\hat{\epsilon} = -\frac{3}{\pi(G-1)(2G-1)} \sum_{g=0}^{G-1} g \cdot \arg([\mathbf{v}]_g) \,. \tag{3.14}$$

To conclude, the estimation of CFO in time domain requires segmenting the signal into G sections, collecting the first L taps of each section, calculating their correlations and finding the largest eigenvalue of the correlation matrix. The overall computational complexity of this process is $\mathcal{O}(G^2L)$. Notice that the first L taps are selected due to their high pilot signal to noise ratio. For most fading channels, a smaller number than L will be sufficient.

3.3 Time-Frequency Combined Estimation

In [2] a frequency domain analysis was used to derive a EVD based estimation of the CFO. The proposed solution in section 3.2 used the last $Q-L$ taps of each section, $\mathbf{y}_g$, to obtain a correlation matrix similar to $\mathbf{Y}^H\mathbf{Y}$ and estimate the CFO using the eigenvector corresponding to the maximal eigenvalue. In this sense, the signal space method proposed in section 3.2 and the noise-space method in [2] are complementary, i.e. each method uses measurement data which is not used in the other. It is thus tempting to combine both methods into one estimation.

3.3.1 Combined Least Squares Estimator

Consider the measurement matrix $\mathbf{Y} = [\mathbf{y}_0, \mathbf{y}_1, \ldots, \mathbf{y}_{G-1}]$, which can be written as $\mathbf{Y} = \mathbf{Y}_I + \mathbf{Y}_{II}$ where $\mathbf{Y}_I = [\mathbf{Y}(1:L,:)^T, \mathbf{0}_{G\times(Q-L)}]^T$ and $\mathbf{Y}_{II} = [\mathbf{0}_{G\times L}, \mathbf{Y}(L+1:Q,:)^T]^T$. The full correlation matrix is,

$$\mathbf{Y}^H\mathbf{Y} = \mathbf{Y}_I^H\mathbf{Y}_I + \mathbf{Y}_{II}^H\mathbf{Y}_{II} + \mathbf{Y}_I^H\mathbf{Y}_{II} + \mathbf{Y}_{II}^H\mathbf{Y}_I\,. \tag{3.15}$$

The last two terms are identically zero, while the first two terms are the so called signal-space (section 3.2) and noise-space [2] correlation matrices. Denote $\hat{\mathbf{R}}_T = \mathbf{Y}_I^H\mathbf{Y}_I$ and $\hat{\mathbf{R}}_F = \mathbf{Y}_{II}^H\mathbf{Y}_{II}$. The corresponding estimated $\boldsymbol{\alpha}$ vectors are denoted $\mathbf{u}_{\max}(\hat{\mathbf{R}}_T)$ and $\mathbf{u}_{\min}(\hat{\mathbf{R}}_F)$ which are the eigenvectors of the maximum and minimum eigenvalues of the appropriate matrices. We now turn to combine the outputs of the methods into one model as,

$$\begin{bmatrix} \arg[\mathbf{u}_{\max}(\hat{\mathbf{R}}_T)] \\ \arg[\mathbf{u}_{\min}(\hat{\mathbf{R}}_F)] \end{bmatrix} = \begin{bmatrix} -\frac{2\pi}{G}\mathbf{g} \\ -\frac{2\pi}{G}\mathbf{g} \end{bmatrix} \epsilon\,. \tag{3.16}$$

By solving the LS problem defined by (3.16) we obtain the estimate,

$$\hat{\epsilon} = -\frac{b}{2}\sum_{g=0}^{G-1} g\left(\arg[\mathbf{u}_{\max}(\hat{\mathbf{R}}_T)]_g + \arg[\mathbf{u}_{\min}(\hat{\mathbf{R}}_F)]_g\right), \tag{3.17}$$

where $b = \frac{3}{\pi(G-1)(2G-1)}$. As might be expected, the combined estimator is a simple arithmetic average between both estimations. A more heuristic approach is a weighted sum of the estimates of the form,

$$\hat{\epsilon} = -b\sum_{g=0}^{G-1} g\left(\beta\arg[\mathbf{u}_{\max}(\hat{\mathbf{R}}_T)]_g + (1-\beta)\arg[\mathbf{u}_{\min}(\hat{\mathbf{R}}_F)]_g\right), \tag{3.18}$$

where $0 \leq \beta \leq 1$. For $\beta = 0.5$ we get the LS solution. An intuitive selection of weights is $\beta = L/Q$, which accounts for the relative number of samples used for each estimate.

3.3.2 Generalized Eigenvalue Decomposition Estimator

As mentioned above, the time-domain estimator attempts to maximize a cost function while the frequency domain estimator tries to minimize an equivalent quantity. A combined model can be proposed to maximize these quantities' ratios. i.e. the optimization problem can be rephrased as a Rayleigh quotient

$$\hat{\boldsymbol{\alpha}}(\epsilon) = \underset{\boldsymbol{\alpha}(\epsilon)}{\operatorname{argmax}} \frac{\boldsymbol{\alpha}^H(\epsilon)\hat{\mathbf{R}}_T\boldsymbol{\alpha}(\epsilon)}{\boldsymbol{\alpha}^H(\epsilon)\hat{\mathbf{R}}_F\boldsymbol{\alpha}(\epsilon)}. \tag{3.19}$$

We thus arrive to a well known generalized eigenvalue problem, which is equivalent to the simple problem of finding the maximal eigenvalue of the matrix $\hat{\mathbf{R}}_F^{-1}\hat{\mathbf{R}}_T$. Finally the generalized eigenvalue decomposition (GEVD) estimator is (applying the same LS solution as in (3.14)),

$$\hat{\epsilon}_{\mathrm{RQ}} = -b\sum_{g=0}^{G-1} g\cdot\arg([\mathbf{u}_{\max}(\hat{\mathbf{R}}_F^{-1}\hat{\mathbf{R}}_T)]_g), \tag{3.20}$$

where $\mathbf{u}_{\max}(\hat{\mathbf{R}}_F^{-1}\hat{\mathbf{R}}_T)$ is the eigenvector corresponding to the largest eigenvalue of $\hat{\mathbf{R}}_F^{-1}\hat{\mathbf{R}}_T$.

3.4 Simulations and Trials

The proposed methods were simulated to illustrate their performances. We used OFDM blocks of $K = 2048$ QPSK symbols with $G = 8$ and bandwidth of $W = K\Delta f = 12.5$ KHz. The normalized CFO was fixed to $\epsilon_0 = 0.2$. First, we considered a channel with $L = 100$

($Q - L = 156$), corresponding to a delay spread of 8 ms with 15 paths of descending amplitudes. We evaluate the root mean square error (RMSE) of the CFO using 5 estimates: (1) Time domain ($\beta = 0$); (2) Frequency domain from [2] ($\beta = 1$); (3) Combined LS ($\beta = 0.5$); (4) Weighted LS ($\beta = L/Q$) and (5) GEVD based. Fig. 3.1 shows the RMSE performance (simulated CIR presented at the bottom). Each value represents statistics of 10,000 trials (a total of 280,000). Clearly, the GEVD based estimator achieves the best results, outperforming the frequency domain estimate in low signal-to-noise ratio (SNR). As expected, when applying the time domain estimate ($\beta = 1$), a noise floor caused by the data tones is reached for high SNR.

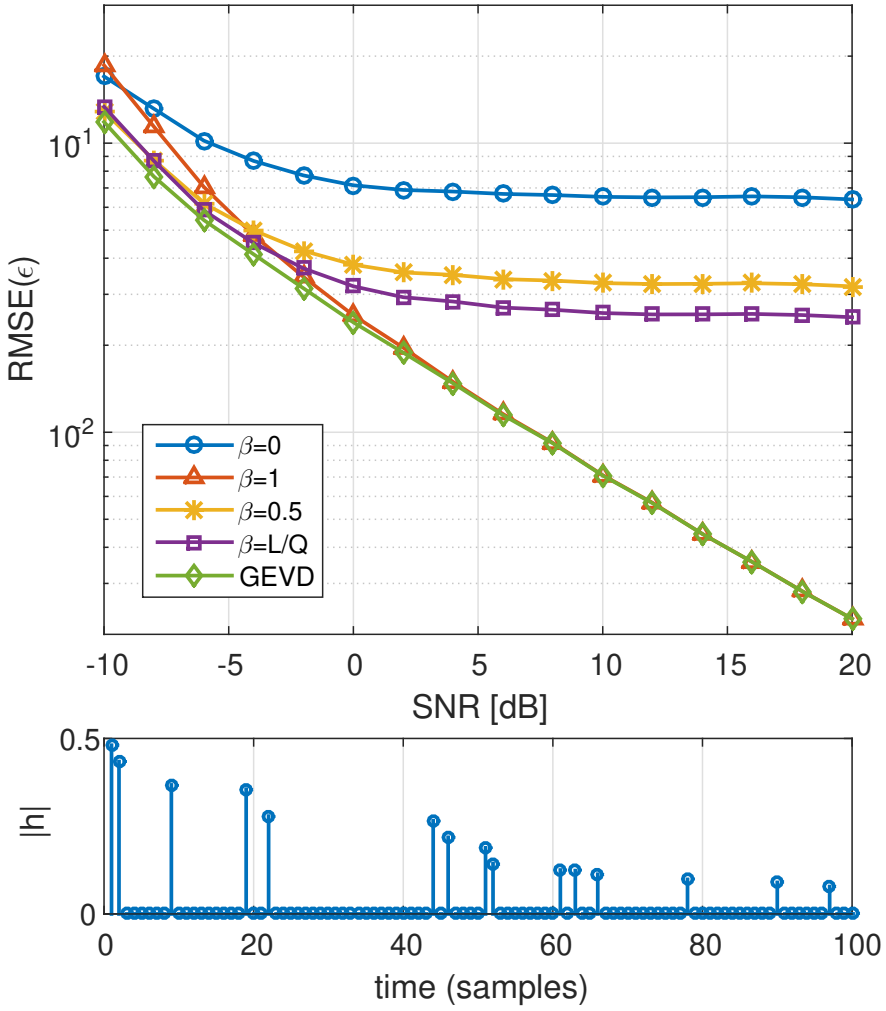

Figure 3.1: RMSE of the CFO estimates versus the SNR of the proposed estimation techniques.

We next turn to investigate the effect of the CIR delay spread on the estimate. Fig. 3.2 shows the RMSE of the CFO estimates as a function of the channel delay-spread in terms of L/Q for a fixed SNR of 3 dB. As expected, the performance degrades for long channels, however the behavior is not the same for frequency and time domain estimations. We deduce that the choosing the best estimator of the proposed solution depends on the expected SNR and CIR, however it seems that the GEVD based estimate illustrates the best performance for all scenarios with price of minor degradation in computational complexity, caused by the $G \times G$ matrix inversion needed (since G is typically small)

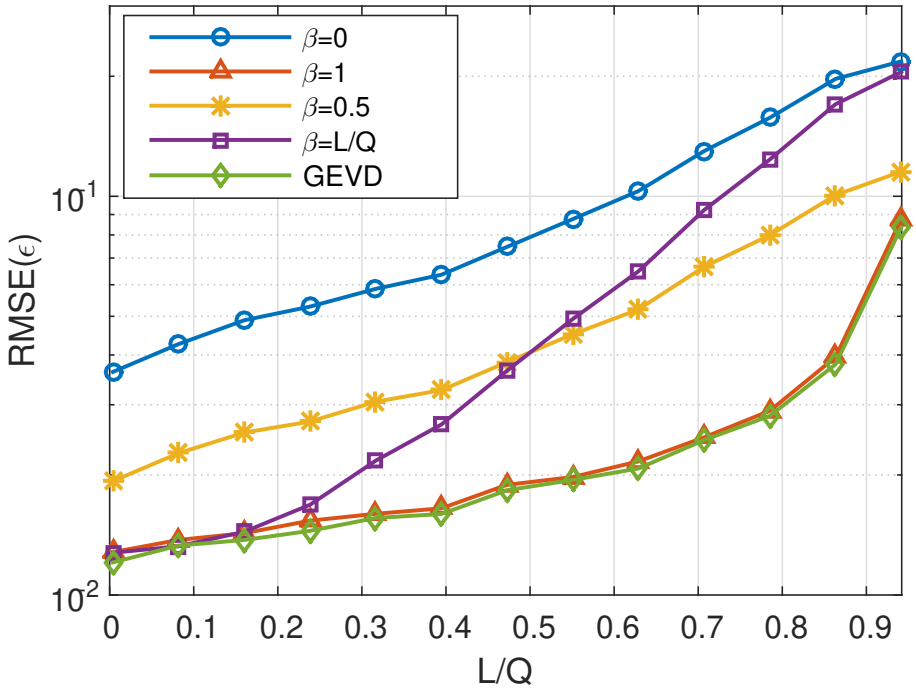

Figure 3.2: RMSE of the CFO estimates versus the CIR delay spread in terms of L/Q.

Pool trials were held in a 10m $\times$ 20m $\times$ 10m acoustic tank. The receiving and transmitting transducers were placed at the center of the pool 2m apart at 3m depth. Since the typical CIR in the tank is fairly long, we used $K = 2048$, $G = 4$ and $L = 250$, i.e. $L/Q = 0.49$. A total of 1400 OFDM blocks were transmitted, including both static and motion scenarios. We compared the proposed methods with the state of the art null carriers CFO estimation [14] (which has higher computational complexity). Overall, the performance witnessed in the pool was consistent with the simulations. Fig. 3.3 shows the CFO estimates of two packets of motion scenarios. In each set a different displacement

was performed. In the top plot, the displacement was large, as can be seen all methods follow the harmonic oscillation of the transducer in the water. The bottom plot illustrates the results of a much subtle displacements. Here we show the differences between the best performing methods (the time domain method produced poor results as was expected in pool trial scenario which is characterized with long delay spread).

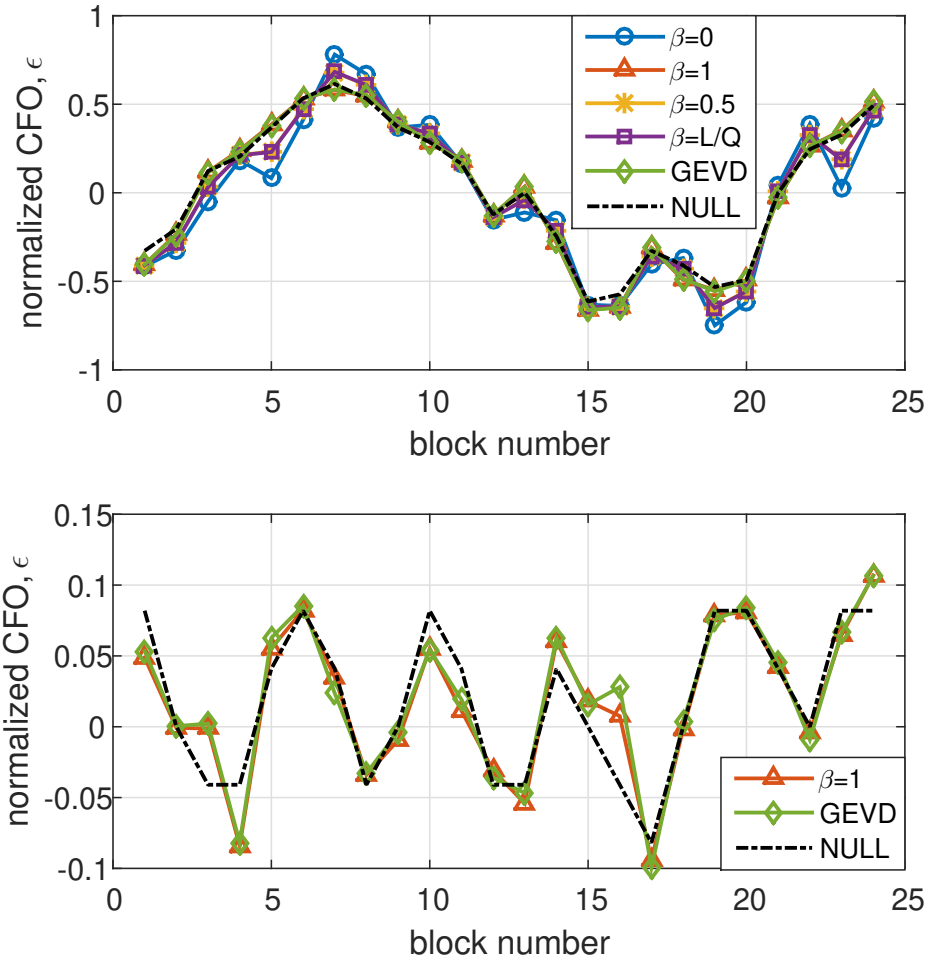

Figure 3.3: CFO estimates of two motion sets in the pool trial.

3.5 Conclusions

We proposed a group of EVD based CFO estimators. The first, can be derived using a frequency domain analysis while the second uses time domain analysis to achieve a complementary estimate. We then proposed to combine the two estimates, first by applying

a LS model on the estimates themselves and then by constructing a unified model that yields one GEVD solution for both problems. Simulations show that the frequency domain estimator has superior performance over the time domain since the latter suffers from non negligible data-tones interference in high SNR. However the unified Rayleigh quotient model achieves the best performance for both high and low SNR. Pool experiments and sea trials further emphasized these performance results. The proposed methods can be easily implemented in low power UAC modems to achieve a low complexity and high performance estimate.

Chapter 4

A Constrained Optimization for Pilots Design

4.1 Introduction

In this chapter we address the transmitter-side drawback of the low-complexity EVD based method. High PAPR is an inherent problem in OFDM systems, resulting in reduction of the effective transmitted power. As such, it has received much attention in the literature, with solutions ranging from the simple clipping-and-filtering [3] to distortion-less techniques [1]. When introducing identical pilots, the already high PAPR increases significantly. We first investigate the cost function of the low-complexity solution [2] in order to explore the affect of the pilot tone design on the ability to estimate the CFO. We then formulate the trade-off between high PAPR and the desire time-locality used for phase estimation. As a result of this analysis, we propose a closed-form algorithm which enables the modem designer to compromise between PAPR and time locality, while guaranteeing the low complexity CFO estimation. Simulations show that the proposed algorithm achieve significant reduction in PAPR, which reaches less than 0.5dB of the classic random-pilots case with only minor effects on the cost function.

4.2 Cost Function Analysis

Notice that the term $\mathbf{F}_Q^H(:, 1:L)\mathbf{D}_p^H\mathbf{F}_Q\mathbf{\Gamma}_Q^H(\epsilon)\mathbf{Y}\boldsymbol{\alpha}(\epsilon)$ in (2.20) describes the L-tap cross correlation between the pilot signal and the CFO compensated sections. In order to better

reflect this observation, we define the pilot-signal cross-correlation operator

$$\mathbf{\Psi} = \mathbf{F}_Q^H \mathbf{D}_p \mathbf{F}_Q(:, 1:L)\,, \tag{4.1}$$

which is a circulant matrix with first column and first row given by $\boldsymbol{\psi} = \text{IFFT}(\text{diag}(\mathbf{D}_p))$ (the time domain pilot signal) and $[\psi(0), \mathbf{0}_{L-1}]$ respectively. The cost function in (2.20) then becomes

$$\ell(\epsilon) = \|\mathbf{Y}\boldsymbol{\alpha}(\epsilon)\|^2 - \boldsymbol{\alpha}^H(\epsilon)\mathbf{Y}^H\mathbf{\Gamma}_Q(\epsilon)\mathbf{\Psi}\mathbf{\Psi}^H\mathbf{\Gamma}_Q^H(\epsilon)\mathbf{Y}\boldsymbol{\alpha}(\epsilon)\,. \tag{4.2}$$

The matrix $\mathbf{\Psi}\mathbf{\Psi}^H$ in (4.2) has the following structure: The top-left $(L + L_p - 1)\times(L + L_p - 1)$ block is defined similarly to $\mathbf{r}_\psi$, the cyclic auto-correlation function of $\boldsymbol{\psi}$, where L_p is the support of $\boldsymbol{\psi}$. The remaining entries of the matrix are equal to zero. Figure 4.1 illustrates the diagonal and off-diagonal of $\mathbf{\Psi}\mathbf{\Psi}^H$ for a few important examples.

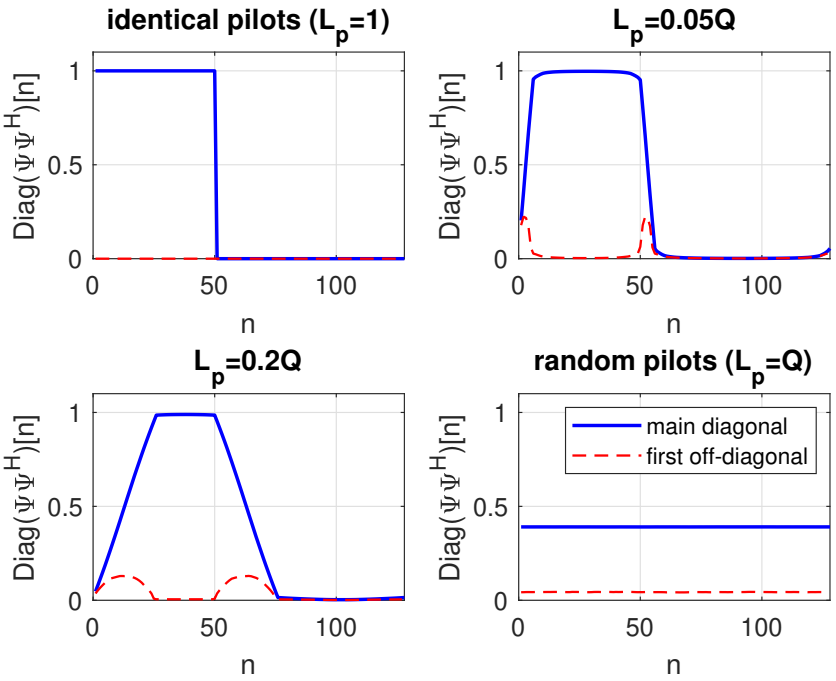

Figure 4.1: Examples of the diagonals of $\mathbf{\Psi}\mathbf{\Psi}^H$ for 4 different L_p values where $Q = 128$ and $L = 50$. The main diagonals are compared to the first off-diagonal.

It can be observed that for identical pilot tones, the pilot signal is a complex Delta function, which means that $L_p = 1$ and the autocorrelation is a real Delta function,

resulting in the structure,

$$\mathbf{\Psi}\mathbf{\Psi}^H = \begin{bmatrix} \mathbf{I}_L & \mathbf{0}_{L\times(Q-L)} \\ \mathbf{0}_{(Q-L)\times L} & \mathbf{0}_{(Q-L)\times(Q-L)} \end{bmatrix}. \tag{4.3}$$

Substituting (4.3) into (4.2) yields the previous result (2.21), which significantly reduces the dimension of the problem from Q to G (notice that the term in (2.21) is a G-order polynomial). When $L_p > 1$ the structure of $\mathbf{\Psi}\mathbf{\Psi}^H$ is affected. As can be seen in Figure 4.1, the non-zero block is contaminated by edge effects. These $(L_p-1)\times(L_p-1)$ sub-blocks in the top-left and bottom-right are a result of cyclic cross correlation of a zero-padded signal. The resulting cost function is

$$\ell(\epsilon) = \|\mathbf{Y}(L+L_p:Q,:)\boldsymbol{\alpha}(\epsilon)\|^2 + r_{L_p}(\epsilon)\,, \tag{4.4}$$

where $r_{L_p}(\epsilon)$ is the cost function residual caused by the two $(L_p-1)\times(L_p-1)$ sub-blocks of $\mathbf{\Psi}\mathbf{\Psi}^H$. It is clear that as we increase L_p, the larger the residual, up to a point where it completely dominates the cost function. This happens when $L_p > Q-L$, as in the case of random pilots. In this case $\ell(\epsilon) = r_Q(\epsilon)$ and a grid search should be performed [14]. For the rest of our analysis we assume that L_p is chosen such that $r_{L_p}(\epsilon) \ll \|\mathbf{Y}(L+L_p:Q,:)\boldsymbol{\alpha}(\epsilon)\|^2$ and thus ignored, resulting in the approximated cost function,

$$\ell_1(\epsilon) \cong \|\mathbf{Y}(L+L_p:Q,:)\boldsymbol{\alpha}(\epsilon)\|^2\,. \tag{4.5}$$

Similarly to the identical-pilot design, the cost function in (4.5) enables a closed form solution. In the next sections we will utilize the generalization from $L_p = 1$ to a carefully designed L_p in order to control the resulting PAPR.

4.3 Time Locality - PAPR Tradeoff in Pilot Tone Design

The key to the closed-form CFO estimator is having an OFDM block with alternating sections of pilot signal and absence of it. In other words, we want to design our pilot tones such that the corresponding time domain signal will have a localized envelope, while having unit amplitude and equi-spaced pilots which maintain a simple channel equalizer [14]. In order to compare the time locality feature of different candidate pilot signals, we introduce the PDR, describing the power ratios in the non-zero areas of the pilot signal.

For a L_p support pilot signal, the PDR is given by

$$\begin{aligned} \text{PDR} &= \frac{\frac{1}{L_p}\sum_{n=1}^{L_p}|s_p(n)|^2}{\sigma_\eta^2}, \\ &= \frac{\frac{K}{L_p}\sum_{n=1}^{L_p}|s_p(n)|^2}{K-Q}. \end{aligned} \tag{4.6}$$

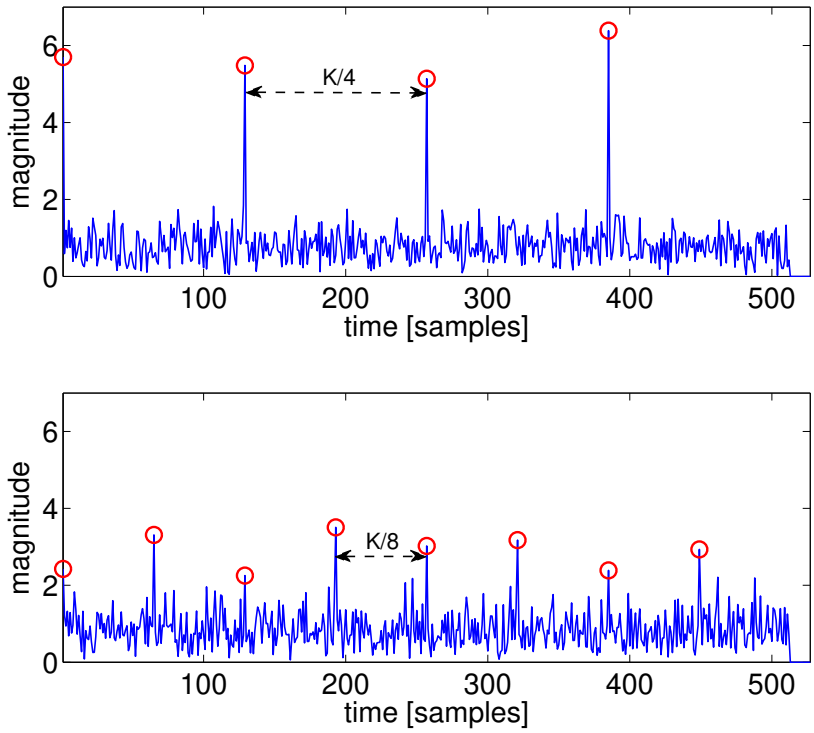

Figure 4.2: Examples of the discrete time OFDM block ($G = 4$ for the upper plot, and $G = 8$ for the bottom plot).

The most trivial and effective pilot design, which meets the requirements is the identical-tone described in (2.8), where $L_p = 1$ and the PDR is $\frac{Q^2}{K-Q}$. Although optimal in terms of time locality, the identical pilot approach causes high PAPR. This is simply due to the contradicting requirements, that while trying to concentrate the time domain pilot signal, we incidentally cause high PAPR. From (2.8) we see that by selecting identical pilots we

obtain a peak value of $\max|s_p(n)| = \frac{Q}{\sqrt{K}}$, therefore the expected value of PAPR is

$$\begin{aligned} E[\text{PAPR}] &= E\left[\frac{\max|x(n)|^2}{\frac{1}{K}\sum_{n=1}^{K}|x(n)|^2}\right], \\ &\cong \left(\frac{Q}{\sqrt{K}} + \sqrt{\frac{K-Q}{K}}\right)^2. \end{aligned} \tag{4.7}$$

In Figure 4.2 we show two transmitted signals for $G = 4$ and $G = 8$. Expectedly from (4.7), as we decrease G, i.e. increase Q, the peak values increase.

4.4 Pilots Design

In order to overcome the increase in PAPR, we propose to re-design the pilot tones in a way that both requirements are met: Localized pilot signal along with reasonably low PAPR. Notice, that unlike classical PAPR reduction schemes, which attempts to reduce the PAPR for the complete block, here we concentrate on reducing the PAPR caused by the pilot-tones in a limited number of taps determined by the CFO estimation algorithm. We start by looking for time domain pilot signals which will allow a compromise between these two contradicting requirements. While identical pilots are highly localized with the worst PAPR, random pilots will have the best PAPR and worst time locality. It is thus suggested to use a windowed envelope for the time domain signal. Ideally, the first L_p taps of the signal will contain all the pilot energy. Note that L_p should be chosen such that $L_p + L < Q$.

The problem we turn to solve now can be defined as follows: We have pilot tones with known unit amplitudes and an unknown phase, denoted by $e^{j\boldsymbol{\phi}}$, and the corresponding time domain signal is constrained by the windowed envelope. This is known as a phase retrieval problem, which has been studied in the past few decades in various fields. The problem was first addressed by Gerchberg and Saxton [10] and later on by Fienup [9], who offered a group of algorithms for solving the problem of recovering a complex image from the measured magnitudes of a real image and far-field Fourier plane in optics. More recently, phase retrieval was suggested for optical imaging [24]. In [28], a pilot tone phase retrieval in OFDM communications was proposed for the receiver side, allowing the transmitter to choose the pilot phases without informing the receiver. Here we use a generalization of the GSA, called the error reduction algorithm [6], to reconstruct the

pilot phases in the transmitter side.

Given the pilot tones in the frequency domain, $e^{j\boldsymbol{\phi}}$ and the desired pilot time domain signal $\mathbf{s}_p$, the problem can be formulated as

$$\begin{aligned} \min_{\boldsymbol{\phi}} \quad & \|\mathbf{s}_p - \boldsymbol{F}_Q^H e^{j\boldsymbol{\phi}}\|^2 \\ \text{s.t.} \quad & s_p(n) = 0, \text{ for } n = L_p + 1, \ldots, Q\,. \end{aligned} \tag{4.8}$$

The error reduction algorithm solves this non-convex problem iteratively by alternating projections. The algorithm transforms the time and frequency domain signals back and forth, where in each such alternation the amplitude constraint is applied (see Algorithm 1). Notice that here we chose a final condition using the error magnitude of the time domain constraint. One may consider other cost functions such as a weighted sum of the achieved PAPR and time domain error. An example of the resulting OFDM block using a rectangular window is presented in Figure 4.3. Here we used $K = 512$ subcarriers, the pilot spacing is $G = 4$ and L_p is chosen to be 10% of the pilot signal period, Q. In this example, the resulting PAPR was 10dB, compared to the identical pilot waveform which results in an expected PAPR of 16.3dB.

Algorithm 1 Constrained Pilots Design

define $\mathbf{W} = \text{diag}[w_1, \ldots, w_{L_p}, 0, \ldots, 0]$
initialize $\boldsymbol{\phi}_0$, $\varepsilon = \infty$, $\mathbf{a}_0 = \text{IFFT}(e^{j\boldsymbol{\phi}_0})$
while $\varepsilon > \eta$ **do**
    $\mathbf{b}_i = \exp\{j \arg[\mathbf{a}_{i-1}]\}$
    $\mathbf{c}_i = \text{FFT}(\boldsymbol{W}\mathbf{b}_i)$ ▷ Applying time domain constraint
    $\mathbf{d}_i = \exp\{j \arg[\mathbf{c}_i]\}$
    $\mathbf{a}_i = \text{IFFT}(\mathbf{d}_i)$
    $\varepsilon = \|a_i[L_p + 1, \ldots, Q]\|^2$
end while
return $\mathbf{d}_i$

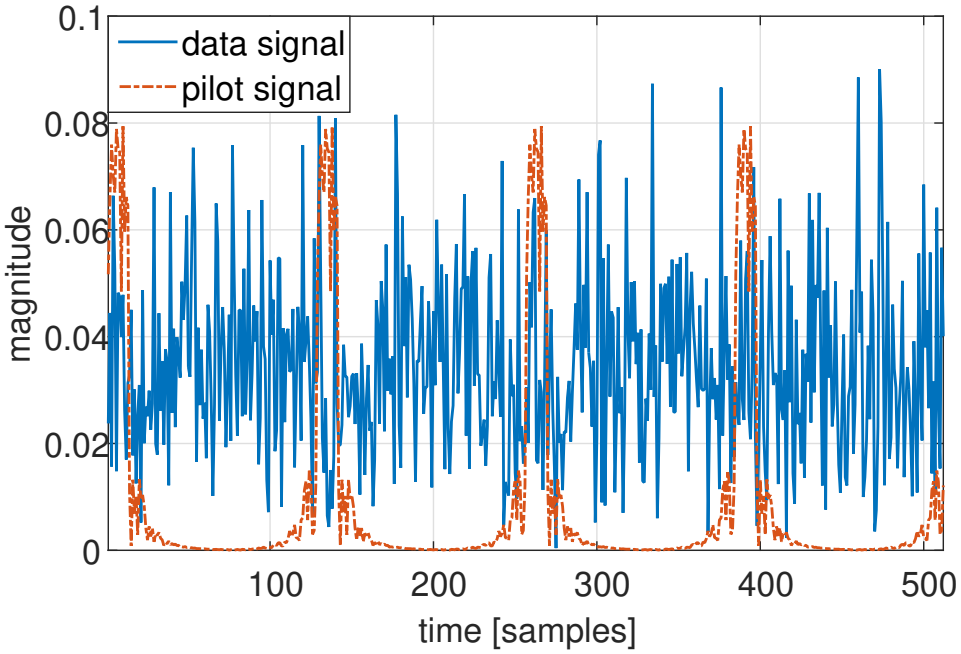

Figure 4.3: Examples of the discrete time OFDM block with $G = 4$ where the pilot tones are designed with the phase retrieval algorithm for $L_p = 0.1Q$.

At this point, we have designed the transmitted waveform, which allows us to use low complexity CFO estimators while controlling the PAPR values. We now turn to design the receiver side CFO estimator.

4.5 Numerical Results

The reduced PAPR scheme presented is analyzed in simulation. Figure 4.4 shows the PAPR complementary cumulative distribution function (CCDF). L_p Values of 1%, 10% and 25% of the section length, $Q = 256$, are compared to the random and identical pilot cases. It can be seen that choosing a window of 10% results in a CCDF of merely 0.8dB from the random pilots case. Depending on the expected channel delay spread, one can choose a window size which will compromise between the resulting PAPR, the channel taps needed and the remaining so-called noise space taps, not affected by the pilots, defined as $L_\epsilon = Q - L_p - L + 1$

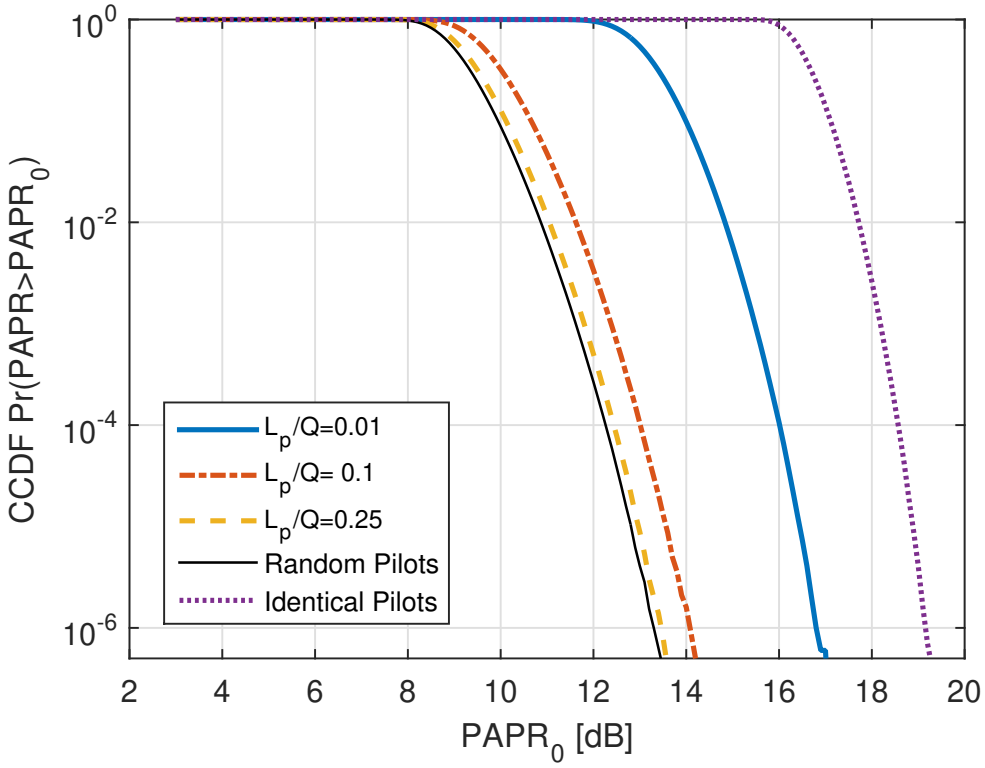

Figure 4.4: CCDF of PAPR for different window sizes

In Section 4.3 we have discussed the trade-off between the PDR and PAPR. While it is quite clear what are the implications of high PAPR, it is important to examine the PDR as well. Figure 4.5 shows the effect of increasing PDR on the estimation error. Simulation is performed using $K = 1024$, $Q = 256$. It can be seen that for high PDR values the estimation error is reasonably small (0.6% of carrier spacing for PDR= 10dB). However, when approaching $Q - L$ the error drastically increases. Interestingly, the generally monotonic curve in Figure 4.5 has a peak at a very high PDR value. This is caused by the large error of Algorithm 1 when working with a very narrow window (in this case 2-3 taps).

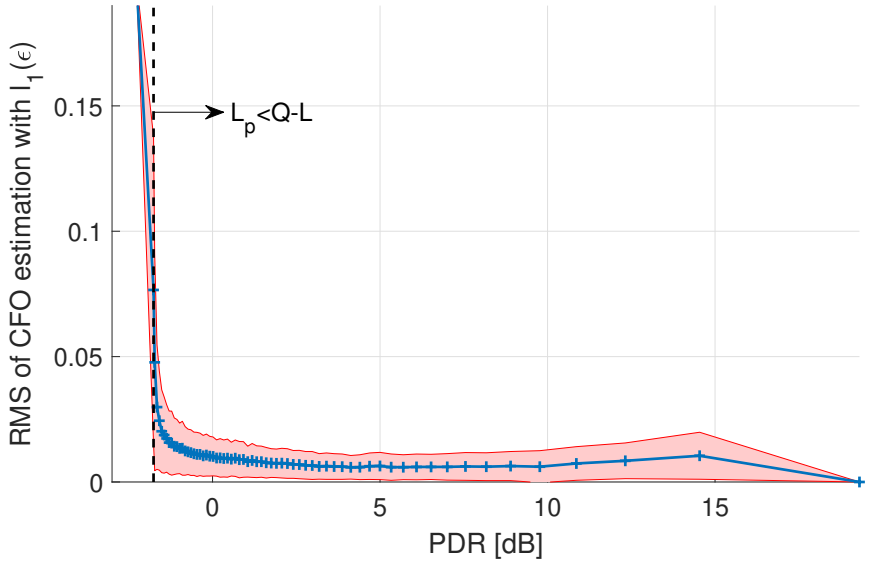

Figure 4.5: Effect of the PDR on the cost function error. The horizontal axis describes the average PDR [dB] while the vertical corresponds to the RMS of the CFO error when using $\ell_1(\epsilon)$ with a grid search, the colored area represents the bounds of the estimation error. When L_p exceeds $Q - L$ (in this case $L = 0.5Q$), the cost function will not have a minimum, as a result, the minimum value will be one of the search grid bounds.

4.6 Conclusions

We considered the problem of reducing the PAPR caused by using identical pilots for CFO estimation. Rather than using existing methods to reduce the PAPR we have looked into the reasons leading to use identical pilots in the first place. We have made the observation that the estimation technique requires periodic segments of high PDR which are achieved by a windowed pilot signal, which is a generalization of the identical pilot tones and its corresponding impulse pilot signal. We have proposed a phase retrieval method based on the GSA algorithm for deigning a windowed pilot signal, while maintaining unit amplitude pilot tones. Simulations show that the reduction in PAPR is significant, bringing it within fractions of dB to the random pilot design, while preserving time locality.

Chapter 5

Time-Varying CFO Estimation

5.1 Introduction

Commonly, OFDM waveforms are designed such that one block duration is shorter than the coherence time of the channel [5]. However, the coherence time may vary between different environments and sea states in such a way that enforcing the block duration to be shorter may cause significant loss of bit rate. In this chapter, we expand our closed-form CFO estimate to a time-varying model. The core idea is that by creating sub-blocks of pilot-signal periods, we are able to observe sub-block variations, which can not be observed with the classic random pilots. This means that instead of having a time scale of T, the block duration, we can now observe variations in the scale of T/G. We present two model-based approaches - the first, assumes that the CFO variation during the block duration can be approximated as a low-order polynomial. In the second solution, we introduce a linear piecewise approach, where the pieces correspond to the pilot-signal segments. As we shall see, these approaches are limited by model pre-conditions that, when met, result in significant performance enhancement.

5.2 Polynomial Model

Let us assume that the CFO is some continuous function in time and, as so, it can be represented by its Taylor polynomial

$$\epsilon[n] = \sum_{l=0}^{\infty} \epsilon_l n^l \quad , \quad 0 \leq n \leq K-1 \,. \tag{5.1}$$

Replacing (5.1) into (1.6) we obtain

$$\mathbf{\Gamma}_P = \mathrm{diag}(1, e^{j\frac{2\pi}{K}\sum_{l=0}^{\infty}\epsilon_l}, \ldots, e^{j\frac{2\pi}{K}[(P-1)\sum_{l=0}^{\infty}\epsilon_l(P-1)^l]}) \,. \tag{5.2}$$

The received signal is defined similarly to (1.5), where $\mathbf{\Gamma}_P$ is determined by a time varying CFO,

$$\mathbf{y} = \mathbf{\Gamma}_P \mathbf{H}\mathbf{T}_{zp}\mathbf{F}_K^H\mathbf{s} + \mathbf{n} \,. \tag{5.3}$$

We now turn to apply the EVD solution to the time varying model. First, we notice that $\hat{\mathbf{R}}$ in (2.24) represents the correlation matrix of the OFDM G segments and thus inherent in this solution. Therefore, we turn to look at the gth section of $\mathbf{y}$, described by $\mathbf{y}_g = \mathbf{\Gamma}_g\mathbf{z}_g + \mathbf{n}_g$, where $\mathbf{z}_g$ is the CFO compensated signal obtained by taking the Q samples of the gth section of $\mathbf{H}\mathbf{T}_{\mathrm{zp}}\mathbf{F}_K^H\mathbf{s}$, and

$$\mathbf{\Gamma}_g = \mathrm{diag}\left[e^{j\frac{2\pi}{K}\sum_{l=0}^{\infty}(gQ)^{l+1}\epsilon_l}, \ldots, e^{j\frac{2\pi}{K}[\sum_{l=0}^{\infty}(gQ+Q-1)^{l+1}\epsilon_l]}\right] . \tag{5.4}$$

Notice that last L taps of $\mathbf{y}$ are discarded since it has no contribution to the CFO estimation as we assume that $L + L_p < Q$. The correlation of any two sections g and g' will give the following expression,

$$\mathbf{y}_g^H\mathbf{y}_{g'} = \mathbf{z}_g^H\mathbf{\Gamma}_g^H\mathbf{\Gamma}_{g'}\mathbf{z}_{g'} + \mathbf{n}_g^H\mathbf{n}_{g'} \,, \tag{5.5}$$

where the elements involving signal and noise products are assumed zero. Let us derive the CFO related term in (5.5),

$$d_{g,g'}[n] = \exp\left\{\frac{j2\pi}{K}\sum_{l=0}^{\infty}\epsilon_l\left[(n+g'Q)^{l+1} - (n+gQ)^{l+1}\right]\right\} \,, \tag{5.6}$$

where $d_{g,g'}[n] = \mathrm{Diag}(\mathbf{\Gamma}_g^H\mathbf{\Gamma}_{g'})[n]$. Notice that each binomial of the term can be represented as,

$$(n+gQ)^l = (gQ)^l + n^l + r_l(n,g) \,, \tag{5.7}$$

where,

$$r_l(n,g) = \sum_{k=1}^{l-1}\binom{l}{k}n^{l-k}(gQ)^k \tag{5.8}$$

is the residual of the binomial decomposition, for instance $r_0(n,g)=0$, $r_1(n,g)=0$, and $r_2(n,g)=2ngQ$. Using this formulation we obtain

$$\begin{aligned} d_{g,g'}[n] &= \underbrace{\exp\left\{-\frac{j2\pi}{G}\sum_{l=1}^{\infty} g^l Q^{l-1}\epsilon_{l-1}\right\}}_{\alpha_g^*}\underbrace{\exp\left\{\frac{j2\pi}{K}\sum_{l=1}^{\infty}\epsilon_l[r_l(n,g')-r_l(n,g)]\right\}}_{\lambda_{g,g'}[n]} \\ &\quad \times\underbrace{\exp\left\{\frac{j2\pi}{G}\sum_{l=1}^{\infty} g'^l Q^{l-1}\epsilon_{l-1}\right\}}_{\alpha_{g'}}, \end{aligned} \tag{5.9}$$

where α_g is the constant inter-section phase accumulation and $\lambda_{g,g'}[n]$ is the difference between phases accumulated within two sections. Next, (5.5) can be written as

$$\mathbf{y}_g^H\mathbf{y}_{g'} = \alpha_g^*\alpha_{g'}\mathbf{z}_g^H\mathbf{\Lambda}_{g,g'}\mathbf{z}_{g'} + \mathbf{n}_g^H\mathbf{n}_{g'}\,, \tag{5.10}$$

where $\mathbf{\Lambda}_{g,g'} = \mathrm{diag}(\lambda_{g,g'}[0],\ldots,\lambda_{g,g'}[Q-1])$. Ideally, the matrix $\mathbf{\Lambda}_{g,g'}$ can be neglected. For zero and first order polynomials $\mathbf{\Lambda}_{g,g'}$ is the identity matrix, in which case we arrive to the cost function (2.16). However, as higher orders are introduced the accumulated phase may not be negligible depending on ϵ_l and G. Therefore, we will omit $\mathbf{\Lambda}_{g,g'}$ when the CFO function can be approximated as linear and the residual is kept small, otherwise it may dominate the cost function. By using the above approximation we obtain the EVD formulation for the polynomial time varying model,

$$\mathbf{y}_g^H\mathbf{y}_{g'} = \alpha_g^*\alpha_{g'}\mathbf{z}_g^H\mathbf{z}_{g'} + \mathbf{n}_g^H\mathbf{n}_{g'}\,. \tag{5.11}$$

Collecting all section correlations into the matrix,

$$\mathbf{R}_{PL} = \mathbf{Y}^H\mathbf{Y}\,. \tag{5.12}$$

Substituting (5.12) into (4.5), we obtain the optimization problem

$$\underset{\boldsymbol{\alpha}}{\mathrm{argmin}}\ \boldsymbol{\alpha}^H\mathbf{R}_{PL}\boldsymbol{\alpha} \quad \text{s.t.} \quad \boldsymbol{\alpha}^H\boldsymbol{\alpha} = G\,, \tag{5.13}$$

where we added the constraint on $\boldsymbol{\alpha}$ in order to guarantee the structure in (2.19). Notice that $\boldsymbol{\alpha}^H\boldsymbol{\alpha} = G$ is a weak constraint, however, it is enough in order to define the equivalent

optimization problem of minimizing the following Rayleigh quotient,

$$R(\mathbf{R}_{PL}, \boldsymbol{\alpha}) = \frac{\boldsymbol{\alpha}^H \mathbf{R}_{PL} \boldsymbol{\alpha}}{\boldsymbol{\alpha}^H \boldsymbol{\alpha}}\,, \tag{5.14}$$

which is minimized by the eigenvector corresponding to the smallest EV of $\mathbf{R}_{PL}$, i.e.

$$\arg[\mathbf{u}_{\min}(\mathbf{R}_{PL})](g) = -\frac{2\pi}{G}\sum_{l=1}^{G-1} g^l Q^{l-1}\epsilon_{l-1} + v_g\,, \tag{5.15}$$

where v_g is assumed to be zero-mean Gaussian noise with unknown variance σ_v^2. Converted to matrix formulation

$$\arg[\mathbf{u}_{\min}(\mathbf{R}_{PL})](g) = -\frac{2\pi}{G}\mathbf{a}_g^T \mathbf{Q}\boldsymbol{\epsilon} + v_g\,, \tag{5.16}$$

where $\mathbf{a}_g = [g, g^2, \ldots, g^{G-1}]^T$, $\mathbf{Q} = \mathrm{diag}(1, Q, \ldots, Q^{G-2})$ and $\boldsymbol{\epsilon} = [\epsilon_0, \epsilon_1, \ldots, \epsilon_{G-2}]^T$. Collecting all G elements of $\boldsymbol{\alpha}$, we obtain

$$\mathbf{r} \equiv \arg[\mathbf{u}_{\min}(\mathbf{R}_{PL})] = -\frac{2\pi}{G}\mathbf{A}\mathbf{Q}\boldsymbol{\epsilon} + \mathbf{v}\,, \tag{5.17}$$

where $\mathbf{A} = [\mathbf{a}_0, \ldots, \mathbf{a}_{G-1}]^T$. Once again, as in the constant CFO case, we arrive to a LS formulation of the problem. As the elements of $\boldsymbol{\alpha}$ represent the phase accumulated between the block sections due to CFO, we use it as a stepping stone towards reconstructing ϵ.

Given the measurement vector $\mathbf{r}$ (obtained by the EVD estimator), the LS problem defined by the polynomial model is given by

$$\hat{\boldsymbol{\epsilon}} = \underset{\boldsymbol{\epsilon}}{\mathrm{argmax}} \left\| \mathbf{r} + \frac{2\pi}{G}\mathbf{A}\mathbf{Q}\boldsymbol{\epsilon} \right\|^2 = -\frac{G}{2\pi}\mathbf{Q}^{-1}(\mathbf{A}^T\mathbf{A})^{-1}\mathbf{A}^T\mathbf{r}\,. \tag{5.18}$$

Notice that due to the structure of $\mathbf{A}$, inverting $\mathbf{A}^T\mathbf{A}$ can be numerically challenging as its eigenvalues grow exponentially. In order to overcome this, we alternate our model by introducing the normalized coefficients $b_l = K^l\epsilon_l$. Since we assume $\epsilon[n] < 1$ (practically, it is sufficient to assume that the CFO is within the order of 1), $b_l < 1$. Replacing the normalized coefficients into (5.17), we have

$$\mathbf{r} = -\frac{2\pi}{G}\underbrace{\mathbf{A}\mathbf{Q}\tilde{\mathrm{K}}}_{\tilde{\mathbf{A}}}\mathbf{b} + \mathbf{v}\,, \tag{5.19}$$

where $\mathbf{b} = [b_0, b_1, \ldots, b_{G-1}]^T$ and $\tilde{\mathrm{K}} = \mathrm{diag}(K^0, K^{-1}, \ldots, K^{-(G-1)})$. By introducing this model alternation, we obtain a more convenient matrix $\bar{\mathbf{A}}$, defined by its (g,l)th element $\bar{\mathbf{A}}_{g,l} = (\frac{g}{G})^l$. Using this formulation in the LS solution we have

$$\hat{\boldsymbol{\epsilon}} = -\frac{G}{2\pi}\tilde{\mathrm{K}}(\bar{\mathbf{A}}^T\bar{\mathbf{A}})^{-1}\bar{\mathbf{A}}^T\mathbf{r}\,. \tag{5.20}$$

5.3 Piecewise Constant Model

As mentioned, the main drawback of the polynomial approach is its disregard of the matrix $\boldsymbol{\Lambda}_{g,g'}$, which incorporates the difference in inner-section phase accumulation of two different sections. Since this is not a constant function, it may introduce a non-negligible effect. Ideally the phase accumulated from one section to another is identical to all samples. Let us consider a piecewise constant model for the time varying CFO as follows,

$$\epsilon[n] = \sum_{g=0}^{G-1} \epsilon_g u_g[n]\,, \tag{5.21}$$

where

$$u_g[n] = \begin{cases} 1, & gQ \le n \le (g+1)Q-1, \\ 0, & \text{otherwise.} \end{cases} \tag{5.22}$$

Substituting (5.21) into (1.6) we obtain $\boldsymbol{\Gamma}_K$ with the received signal being $\mathbf{y} = \boldsymbol{\Gamma}_K\mathbf{H}\mathbf{T}_{\mathrm{zp}}\mathbf{F}_K^H\mathbf{s}+\mathbf{n}$. Following the same steps leading to (5.6), we obtain the CFO related term of the inter-section correlation,

$$\begin{aligned} d[n] &= \exp\left\{\frac{j2\pi}{K}\left[\epsilon_{g'}(n+g'Q) - \epsilon_g(n+gQ)\right]\right\}, \\ &= \underbrace{\exp\left\{-\frac{j2\pi}{G}\epsilon_g g\right\}}_{\alpha_g^*}\underbrace{\exp\left\{\frac{j2\pi}{K}(\epsilon_{g'}-\epsilon_g)n\right\}}_{\lambda_{g,g'}[n]}\underbrace{\exp\left\{\frac{j2\pi}{G}\epsilon_{g'}g'\right\}}_{\alpha_{g'}}. \end{aligned} \tag{5.23}$$

Once again we encounter the inner-section phase accumulation difference (PAD), which can be at most $\frac{2\pi}{K}|\epsilon_{g'} - \epsilon_g|(Q-1)$. The inter-section PAD, however, is at least $\frac{2\pi}{K}|\epsilon_{g'} - \epsilon_g|Q$. Here, we neglect the inner-section PAD. Notice that not correlating adjacent sections and/or trimming the end of each section will further weaken the effect of inner-section PAD. The EVD-estimator of the piecewise constant model yields

$$\arg[\mathbf{u}_{\min}(\mathbf{R}_{PWC})](g) = -\frac{2\pi}{G}\epsilon_g g + v_g\,. \tag{5.24}$$

Collecting all G elements of $\boldsymbol{\alpha}$ we obtain

$$\mathbf{r} \equiv \arg[\mathbf{u}_{\min}(\mathbf{R}_{PL})] = -\frac{2\pi}{G}\mathbf{G}\boldsymbol{\epsilon} + \mathbf{v}\,, \tag{5.25}$$

where $\mathbf{G} = \mathrm{diag}(0, 1, \ldots, G-1)$ and $\boldsymbol{\epsilon} = [\epsilon_0, \ldots, \epsilon_{G-1}]^T$. The LS solution of (5.25) is

$$\hat{\boldsymbol{\epsilon}} = -\frac{G}{2\pi}\boldsymbol{G}^{-1}\mathbf{r}\,. \tag{5.26}$$

The vector $\mathbf{r}$ collects all inter-section phase accumulations with an arbitrary initial phase. In order to achieve the PAD needed for the estimation, we need to shift the phase according to the first element (in other words taking the phase derivative). By doing so, we are left with zero in the first element of $\mathbf{r}$, meaning that ϵ_0 cannot be estimated. One can use the remaining $G-1$ non zero elements to estimate ϵ_0 with various methods. In our implementation, we choose to use the following weighted sum,

$$\hat{\epsilon}_0 = \frac{\sum_{g=1}^{G-1}(G-g)^2\hat{\epsilon}_g}{\sum_{g=1}^{G-1} g^2}\,, \tag{5.27}$$

which is essentially an extrapolation operation. Another possible approach is compensating for the $G-1$ estimated sections and then conducting a one-dimensional search for ϵ_0.

5.4 Simulations Results

We evaluate the performance of the proposed estimates using numerical simulations. We used OFDM blocks of $K = 2048$ QPSK symbols with $G = 8$ and bandwidth of $W = K\Delta f = 12.5$ KHz. The simulated channel was produced using a geometrical model of a shallow water environment. The receiver and transmitter were located 2000m apart at a depth of 5m and 4m, and the seabed set to 70m. The geometrical model included 10 paths with random phases [17]. The delay spread was set to 30ms. Time varying frequency offsets of two types were simulated: (1) polynomial time-variation of order 4, where the coefficients were randomly drawn from the uniform distribution $b_l \sim \mathcal{U}[-0.25, 0.25]$; (2) sinusoidal time-variation of the form

$$\epsilon(n) = \Delta f\left[A_0 + A\sin(2\pi n\frac{f_{\sin}}{K})\right]\,, \tag{5.28}$$

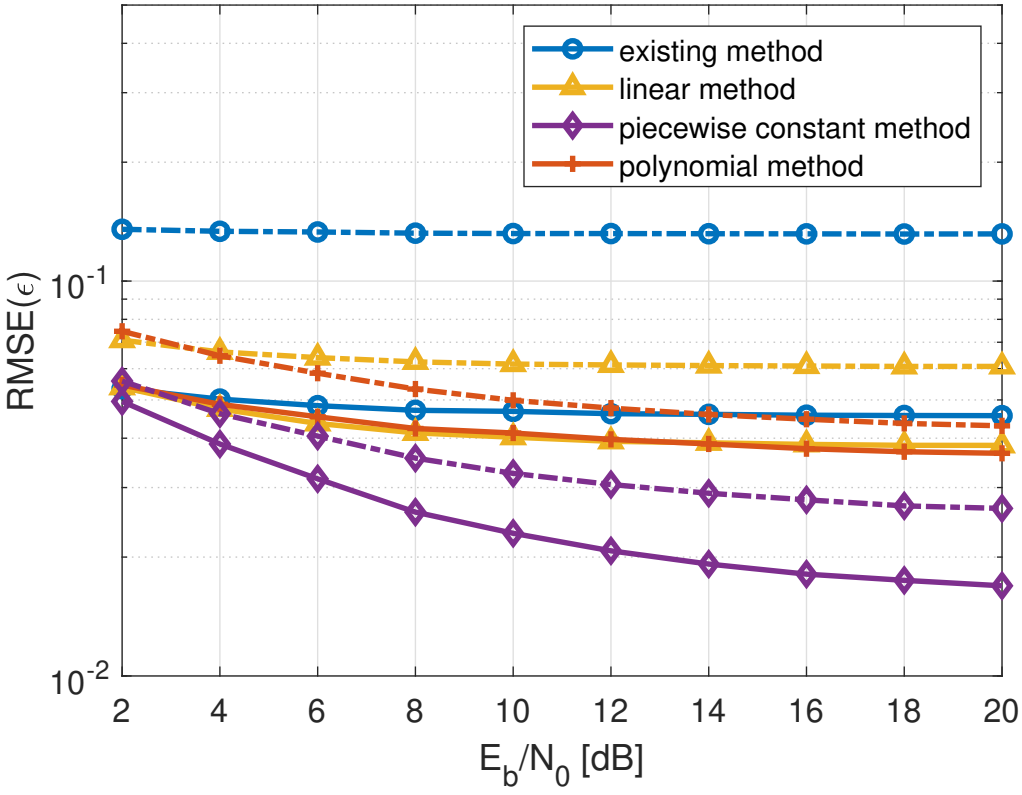

Figure 5.1: RMSE of time-varying CFO estimators. Results for a sinusoidal time-variation are depicted in solid lines while dashed lines correspond to the polynomial time-variation.

where $A_0, A \sim \mathcal{U}[-0.25, 0.25]$ and $f_{\sin} \sim \mathcal{U}[0.25, 2]$. The time varying and constant CFO estimators were simulated over the models and compared. Figure 5.1 presents the RMSE of CFO estimation versus the SNR. The solid lines represent the results for the sinusoidal CFO, which in this case have lower error compared to the polynomial CFO, represented in dashed line. As can be seen, the piecewise-constant estimator's error is consistently lower than this of the linear estimator, which in turn, is lower than the previously published constant CFO estimator. However, the polynomial estimation model achieves inferior results, which in the sinusoidal case is even worst than the constant model. This is due to the approximation of (5.10) which apparently does not hold in this simulation. Figure 5.2 shows how the CFO estimation error ultimately reflects to the BER performance. What has appeared to be an incremental improvement in the CFO accuracy is translated to significant improvement in system performance, which in this case reached up to 9dB for the sinusoidal CFO and a make-or-brake for the polynomial CFO.

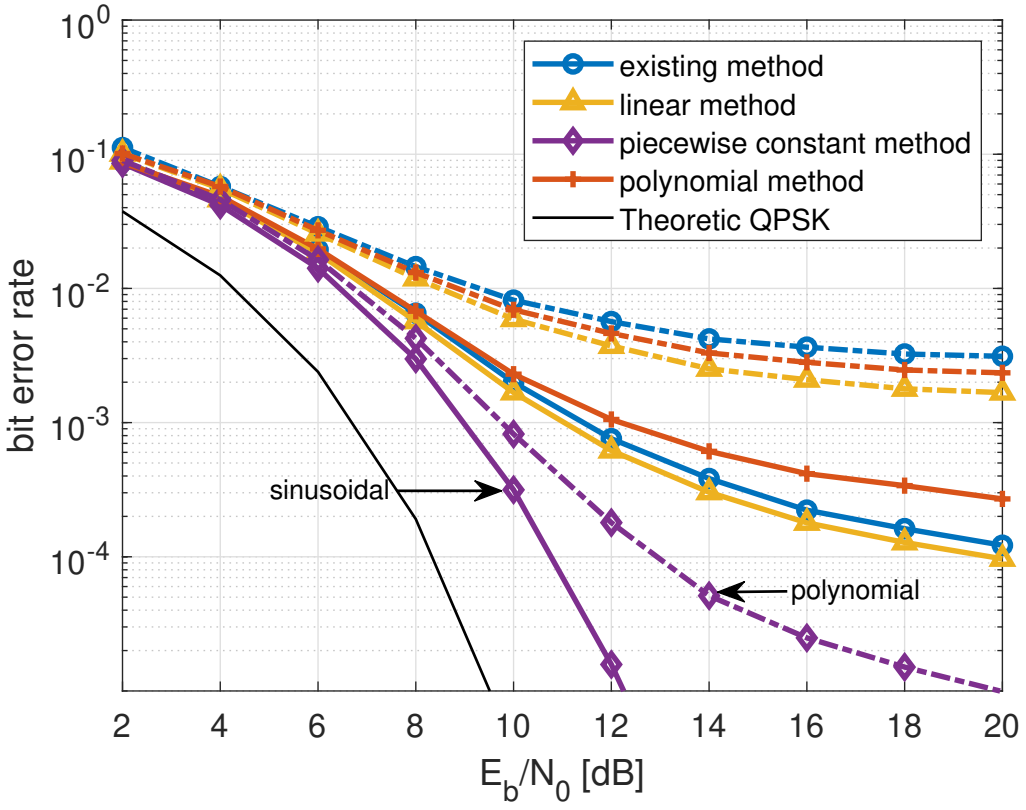

Figure 5.2: Bit error rate of time-varying CFO estimators.

5.5 Conclusions

We have presented a closed-form CFO estimation scheme for underwater acoustic communication with time-varying channels. We have expanded the previously suggested closed-form CFO estimator to include a model-based estimator for rapidly changing frequency offsets. We have suggested two models for the temporal behavior of the CFO which may be used according to the expected environment. The proposed methods are limited by both the assumed temporal behavior model and the number of segments, G. However, under these realistic limitations the performance enhancement may be significant. Simulations show that assuming complex frequency variation models (starting from constant, through linear and piecewise linear) can be translated into BER reduction using the proposed method.

Chapter 6

Conclusions

6.1 Summary

We have considered the problem of estimating the CFO of multicarrier communication in the underwater acoustic channel. We focused the effort on an existing closed-form solution for the problem and have addressed fundamental flaws in the proposed method, which made it impractical.

We have started by expanding the previous solution, by including the pilot-related (signal space) samples in addition to the previously used noise-space samples. By this we introduce more information into the estimator and utilize the complete OFDM block. Using merely the so-called signal-space samples has proved to be insufficient. We have developed two methods in which the noise and signal space samples can be combined - the first, combines the LS estimation phase while the second methods defines a generalized EVD problem in the first step. Both methods have shown to achieve improved performance, while the latter GEVD method was consistently the best performing.

We then turned to solve the problem of high PAPR introduced by using identical pilots for the closed-form CFO estimation. We have shown that the reason for using identical pilots is the need to create a periodic time-domain pilot signal, where the identical pilots create an impulse train. We have then claimed that using other pilot designs may result in the desired periodic feature while maintaining time separation between signal (pilot and data) and noise (data only) samples. This has led us to develop a phase retrieval algorithm, where we design the pilot tone phase to achieve the desired temporal behavior. This has proven to achieve a significant reduction in PAPR while having negligible effect on the CFO estimation.

Finally, we addressed the practical case of time-varying CFO estimation. The previously presented methods have estimated a constant CFO using the correlations of G segments of the OFDM block. We have suggested to use the segment-by-segment correlations to estimate a vector of $G-1$ CFO values. We suggested to model-based methods for the temporal behavior of the CFO between the segments. Simulation results have shown significant performance enhancement number of test cases. By using the time-varying technique, we have allowed the block duration, previously limited by coherence time, to increase by a factor of $G-1$.

The complete transmitter-receiver design allows a low-complexity closed-form solution which is applicable for the real-world UAC dynamic environment. Simulation, as well as pool trial results have shown this potential.

6.2 Future Research

The work presented in this thesis can be further extended in a number of interesting directions:

1. In this work we assumed that the CIR is constant while the CFO may be changing during the block duration. In practice, the CIR may be changing as well. Furthermore, each path in the CIR may change independently causing a Doppler spread. Previous works in multicarrier underwater acoustic communication have made the same assumption. However, when considering the sub-block variations this may not hold. It would be interesting to examine and, if necessary, adjust the proposed methods for a CFO-CIR time-varying channel.

2. In Chapter 4 we have proposed an algorithm which reduces the PAPR caused by the pilot tones. While this reduces the high peaks caused by the use of identical pilots, it does not address the overall problem of high PAPR caused mainly bu the data tones. Previous methods have been suggested to design both the pilot and data tones in order to reduce the block PAPR. It would be tempting then to try to combine these methods to a full transmitter design.

3. The suggested methods can be tested in sea trials. The underwater acoustic channel models commonly used in simulations may be over-simplified compared to the sea environment, as they do not represent all the phenomena typical for this channel

(such as multipath time variations). Pool trials are also limited in their representation of the UAC, as they suffer from longer delay spreads, significant multipath from the surrounding walls and non-realistic time variations. As such, the ultimate validation of the proposed methods in this thesis would be in a carefully controlled sea trial.

4. The time varying algorithm suggested in Chapter 5 is shown to work when the model assumptions are met and reduced dramatically when they are not. It would be interesting to include a channel sensing algorithm which will help make the decision as to which model to use (polynomial, piecewise linear or constant). Alternatively, these models may be triggered in parallel and a technique to choose the best performing methods may be applied post-estimation.

5. As evident from the numerical results, the polynomial model time-varying estimation performance is affected by the assumed polynomial order. We suggest to consider model-order estimation, which will match the model to the measurements. This may increase the overall performance.

Bibliography

[1] A. Amar and G. Avrashi, "Adaptive out-of-band tone selection for peak reduction in underwater multi-carrier acoustic communication," in *OCEANS 2014-TAIPEI*. IEEE, 2014, pp. 1–4.

[2] A. Amar, G. Avrashi, and M. Stojanovic, "Low complexity residual Doppler shift estimation for underwater acoustic multicarrier communication," *IEEE Transactions on Signal Processing*, vol. 65, no. 8, pp. 2063–2076, 2016.

[3] J. Armstrong, "Peak-to-average power reduction for OFDM by repeated clipping and frequency domain filtering," *Electronics Letters*, vol. 38, no. 5, pp. 246–247, 2002.

[4] S. Attallah, "Blind estimation of residual carrier offset in OFDM systems," in *IEEE 5th Workshop on Signal Processing Advances in Wireless Communications, 2004.* IEEE, 2004, pp. 74–77.

[5] Y. M. Aval and M. Stojanovic, "Differentially coherent multichannel detection of acoustic OFDM signals," *IEEE Journal of Oceanic Engineering*, vol. 40, no. 2, pp. 251–268, 2014.

[6] H. H. Bauschke, P. L. Combettes, and D. R. Luke, "Phase retrieval, error reduction algorithm, and Fienup variants: a view from convex optimization," *Journal of the Optical Society of America A*, vol. 19, no. 7, pp. 1334–1345, 2002.

[7] P. C. Carrascosa and M. Stojanovic, "Adaptive channel estimation and data detection for underwater acoustic MIMO-OFDM systems," *IEEE Journal of Oceanic Engineering*, vol. 35, no. 3, pp. 635–646, 2010.

[8] F. Classen and H. Meyr, "Frequency synchronization algorithms for OFDM systems suitable for communication over frequency selective fading channels,"

in *Proceedings of IEEE Vehicular Technology Conference (VTC)*. IEEE, 1994, pp. 1655–1659.

[9] J. R. Fienup, "Reconstruction of an object from the modulus of its Fourier transform," *Optics Letters*, vol. 3, no. 1, pp. 27–29, 1978.

[10] R. W. Gerchberg, "A practical algorithm for the determination of phase from image and diffraction plane pictures," *Optik*, vol. 35, pp. 237–246, 1972.

[11] J. Han, L. Zhang, Q. Zhang, and G. Leus, "Eigendecomposition-based partial FFT demodulation for differential OFDM in underwater acoustic communications," *IEEE Transactions on Vehicular Technology*, vol. 67, no. 7, pp. 6706–6710, 2018.

[12] S. Kay, "A fast and accurate single frequency estimator," *IEEE Transactions on Acoustics, Speech, and Signal Processing*, vol. 37, no. 12, pp. 1987–1990, 1989.

[13] N. Lashkarian and S. Kiaei, "Class of cyclic-based estimators for frequency-offset estimation of OFDM systems," *IEEE Transactions on Communications*, vol. 48, no. 12, pp. 2139–2149, 2000.

[14] B. Li, S. Zhou, M. Stojanovic, L. Freitag, and P. Willett, "Multicarrier communication over underwater acoustic channels with nonuniform Doppler shifts," *IEEE Journal of Oceanic Engineering*, vol. 33, no. 2, pp. 198–209, 2008.

[15] H. Liu and U. Tureli, "A high-efficiency carrier estimator for OFDM communications," *IEEE Communications Letters*, vol. 2, no. 4, pp. 104–106, 1998.

[16] M. Luise, M. Marselli, and R. Reggiannini, "Low-complexity blind carrier frequency recovery for OFDM signals over frequency-selective radio channels," *IEEE Transactions on Communications*, vol. 50, no. 7, pp. 1182–1188, 2002.

[17] X. Lurton, *An Introduction to Underwater Acoustics: Principles and Applications*. Springer Science & Business Media, 2002.

[18] X. Ma, C. Tepedelenlioglu, G. B. Giannakis, and S. Barbarossa, "Non-data-aided carrier offset estimators for OFDM with null subcarriers: Identifiability, algorithms, and performance," *IEEE Journal on Selected Areas in Communications*, vol. 19, no. 12, pp. 2504–2515, 2001.

[19] P. H. Moose, "A technique for orthogonal frequency division multiplexing frequency offset correction," *IEEE Transactions on Communications*, vol. 42, no. 10, pp. 2908–2914, 1994.

[20] M. Morelli and U. Mengali, "An improved frequency offset estimator for OFDM applications," in *1999 IEEE Communications Theory Mini-Conference*. IEEE, 1999, pp. 106–109.

[21] ——, "Carrier-frequency estimation for transmissions over selective channels," *IEEE Transactions on Communications*, vol. 48, no. 9, pp. 1580–1589, 2000.

[22] B. Muquet, Z. Wang, G. B. Giannakis, M. De Courville, and P. Duhamel, "Cyclic prefixing or zero padding for wireless multicarrier transmissions?" *IEEE Transactions on Communications*, vol. 50, no. 12, pp. 2136–2148, 2002.

[23] T. M. Schmidl and D. C. Cox, "Robust frequency and timing synchronization for OFDM," *IEEE Transactions on Communications*, vol. 45, no. 12, pp. 1613–1621, 1997.

[24] Y. Shechtman, Y. C. Eldar, O. Cohen, H. N. Chapman, J. Miao, and M. Segev, "Phase retrieval with application to optical imaging: a contemporary overview," *IEEE Signal Processing Magazine*, vol. 32, no. 3, pp. 87–109, 2015.

[25] M. Stojanovic and J. Preisig, "Underwater acoustic communication channels: Propagation models and statistical characterization," *IEEE Communications Magazine*, vol. 47, no. 1, pp. 84–89, 2009.

[26] U. Tureli, H. Liu, and M. D. Zoltowski, "OFDM blind carrier offset estimation: ESPRIT," *IEEE Transactions on Communications*, vol. 48, no. 9, pp. 1459–1461, 2000.

[27] J.-J. Van de Beek, M. Sandell, and P. O. Borjesson, "ML estimation of time and frequency offset in OFDM systems," *IEEE Transactions on Signal Processing*, vol. 45, no. 7, pp. 1800–1805, 1997.

[28] P. Walk, H. Becker, and P. Jung, "OFDM channel estimation via phase retrieval," in *2015 49th Asilomar Conference on Signals, Systems and Computers*. IEEE, 2015, pp. 1161–1168.

[29] Z. Wang and G. B. Giannakis, "Wireless multicarrier communications where Fourier meets Shannon," *Department of ECE, University of Minnesota, Minneapolis MN*, pp. 1–21, 2000.

[30] Y. Yao and G. B. Giannakis, "Blind carrier frequency offset estimation in SISO, MIMO, and multiuser OFDM systems," *IEEE Transactions on Communications*, vol. 53, no. 1, pp. 173–183, 2005.

[31] Q. Zhan and H. Minn, "New integer normalized carrier frequency offset estimators," *IEEE Transactions on Signal Processing*, vol. 63, no. 14, pp. 3657–3670, 2015.

עבור כל סמל בנפרד כבעיה בעלת פתרון סגור ובתנאי שהסחת התדר נשארת קבועה למשך זמן הסמל. אולם, משערכים אלו סובלים משני חסרונות אשר מונעים את שילובם במערכות תקשורת תת מימיות: הראשון, שימוש בתדרי אימון בעלי פאזה ואמפליטודה זהים מייצרים שיאים מקומיים באות המתבטאים ביחס שיא להספק ממוצע (PAPR) גבוה. שנית, ההנחה כי הסחת התדר הינה קבועה למשך זמן הסמל מגבילה את תכן אות השידור.

בעבודה זו אנו מציגים קבוצה של משערכי תדר יעילים חישובית המתגברים על חסרונות הטכניקות הקודמות ובכך ניתנות ליישום במודמים תת מימיים. בצד המשדר, אנו מציגים שיטה לתכנון תדרי האימון כך שתכונת המחזוריות נשמרת ובד בבד ערכי ה־PAPR נותרים נמוכים. שיטה זו נסמכת על ההבחנה כי התכונה המחזורית הרצויה משיתה אילוץ על מעטפת האות הזמני בעוד שמירה על יחס PAPR נמוך משיתה אילוץ על הפאזה של תדרי האימון. בהתאם לכך, תכן אותות האימון מוגדר כבעית שחזור פאזה, לה קיימים פתרונות מתחומים שונים.

בצד המקלט, אנו מפתחים משערכי תדר אשר מרחיבים את הפתרון הסגור שהוצג לעיל בשני מובנים: ראשית, בניגוד לפתרונות הקודמים בהם נעשה שימוש בדגימות בהן אין נוכחות של תדרי האימון, כלומר מרחב הרעש של סמל ה־OFDM, אנו משתמשים בכלל הדגימות ובכך משיגים שיפור בביצועי המשערך. שנית, אנו מנצלים את העובדה כי אות האימון מכיל מספר מחזורים במשך זמן הסמל על מנת לשערך הסחת תדר המשתנה בזמן. תוצאות נומריות מראות כי עבור ערוצים בעלי מאפייני השתנות זמנית, משערך הסחת התדר שפותח משיג קצב שגיאת סיביות (BER) נמוך משמעותית ביחס לשיטות קודמות. בנוסף, אנו מראים כי תכן המשדר שפותח משיג ערכי PAPR המתקרבים עד כדי חלקי dB לזה המושג במערכות בעלות תדרי אימון אקראיים. זאת, ללא התפשרות על ביצועי משערך הסחת התדר.

תקציר

בעבודה זו אנו מתמקדים בקבוצה של פתרונות סגורים עבור בעיית שערוך הסחת התדר במערכות תקשורת אקוסטית תת־מימית, העושות שימוש באפנון רב־תדרי מסוג OFDM. בשנים האחרונות, בשל תהליכים כגון ההתחממות הגלובלית וניצול משאבים טבעיים, ישנה צמיחה משמעותית בדרישה לטכנולוגיות תת־ימיות. בהתאם לכך, הסביבה התת־מימית קולטת מערכות עתירות מידע עבור מגוון יישומים, ביניהם ניטור סביבתי, הפעלת כלים בלתי מאויישים תת מימיים וכן תקשורת נתונים בין כלים מאויישים. מחד, יישומים אלה דורשים יכולות תקשורת רחבות סרט המאפשרות העברת פקודות שליטה ובקרה ושליחת תמונות ווידאו. מאידך, התווך התת־מימי מהווה אתגר משמעותי עבור קיום תקשורת רחבת סרט. בשל אתגר זה, המחקר המדעי, כמו גם הפתרונות הקיימים, מתמקדים בערוץ האקוסטי כפתרון המועדף לתקשורת בטווחים בינוניים־ארוכים. בתוך כך, בעשור האחרון ניתנה תשומת לב ניכרת לסכמות תקשורת רב־תדריות באפנון OFDM, אשר מאפשרות להתמודד עם אתגרי הערוץ האוקסטי המתאפיין בהשתנות זמנית ובתופעת רב־נתיב.

אחד החסרונות המשמעותיים של תקשורת OFDM הינו רגישותו להסחת התדר הנושא (CFO). תופעה זו עלולה לגרום להפרעה בין־תדרית אשר פוגעת בביצועי המפענח. על מנת להתגבר על חסרון זה, פותחו בעשורים האחרונים מספר טכניקות לשערוך ופיצוי הסחת התדר במערכות OFDM, כאשר עיקר המחקר עוסק במערכות תקשורת אלקטרומגנטית בהן הערוץ שונה מזה האקוסטי. בפרט, הישתנותו הזמנית של הערוץ האקוסטי התת־מימי אינה זניחה ביחס למהירות ההתפשטות בתווך, זאת בנוסף על תופעת הרב־נתיב אשר תוארה לעיל. כתוצאה מתופעות אלה, הסחות התדר בערוץ האקוסטי הינן לא אחידות ומשתנות בזמן. שינויים תדירים אלה מגבילים את מתכנני המודמים האקוסטיים הן לסמלי תקשורת קצרים והן לטכניקות בהן הסחת התדר משוערכת לכל סמל OFDM בנפרד, דבר המצריך חיפוש במערך של היפותזות ובשל כך דורש משאבי חישוב מרובים.

לאחרונה, הוצגו מספר משערכי הסחת תדר עבור תקשורת OFDM תת־מימית אשר מייתרים את הצורך בחיפוש על פני היפותזות ובכך משיגים יעילות חישובית גבוהה. משערכים אלה משתמשים בתדרי אימון בעלי מרווחי תדר קבועים וכן פאזה ואמפליטודה קבועים. כתוצאה מכך מתקבל סמל OFDM המורכב מסכום של אות מידע אקראי ואות אימון מחזורי, כאשר משך המחזור בדגימות זהה למספר תדרי האימון. על־ידי הוספת תכונת המחזוריות, ניתן להגדיר את בעיית שערוך הסחת התדר

תודות

המחקר נעשה בהנחיית פרופ' ישראל כהן וד"ר אלון עמר בפקולטה להנדסת חשמל. ברצוני להודות לשניהם על ההנחיה, ההדרכה והתמיכה בכל שלבי המחקר.

ברצוני להודות לד"ר יעקב בוכריס על התמיכה והסיוע במהלך כל שלבי המחקר.

ברצוני להודות לאישתי יעל, עבור האהבה, העידוד והתמיכה הבלתי פוסקים.

שערוך הסטת תדר משתנה בזמן בתקשורת אקוסטית תת מימית רב־תדרית

חיבור על מחקר

לשם מילוי חלקי של הדרישות לקבלת התואר

מגיסטר למדעים בהנדסת חשמל

גילעד אברשי

הוגש לסנט הטכניון – מכון טכנולוגי לישראל

תמוז תש"פ חיפה יולי 2020

שערוך הסטת תדר משתנה בזמן בתקשורת אקוסטית תת מימית רב־תדרית

גילעד אברשי